METEOR-Berichte

Circulation variability and heat budget off Angola and Namibia

Cruise No. 120

October 17 – November 18, 2015
Recife (Brazil) – Walvis Bay (Namibia)

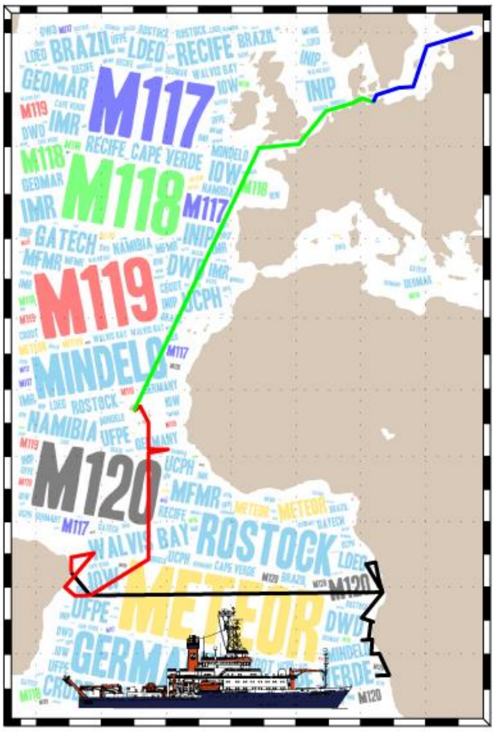

Marcus Dengler, Christian Begler, Sebastian Beier, Florian Cordes, Tina Dippe, Michael Glockzin, Toralf Heene, Carola Heitmann-Bacza, Tim Junker, Thilo Klenz, Robert Kopte, Gerd Logemann, Jan Lüdke, Volker Mohrholz, Soren Nielsen, Marek Ostrowski, Helen Pillar, Andreas Raeke, Ann Katrin Seemann

GEOMAR Helmholtz-Zentrum für Ozeanforschung Kiel

Editorial Assistance:

DFG-Senatskommission für Ozeanographie
MARUM – Zentrum für Marine Umweltwissenschaften Bremen

2015

Table of Content

1 Summary

A physical-biogeochemical survey was carried out in the eastern boundary upwelling region off Angola and Namibia. The research program was an integral component of the EU collaborative project PREFACE ("Enhancing prediction of tropical Atlantic climate and its impacts") and the BMBF-Verbundvorhaben SACUS ("Southwest African Coastal Upwelling System and Benguela Niños"). The major aim of the cruise was (1) to determine the variability of eastern boundary current transport, water masses variability and wave propagation along the coastal wave guide; (2) to quantify physical processes controlling the mixed-layer heat and freshwater budget in the eastern boundary region, including the loss of heat due to turbulent mixing; and (3) to investigate upper-ocean water mass variability associated with the variability of the meridional overturning circulation along a transatlantic transect at 12°S. Altogether, nine moorings with instrumentation observing the variability of currents, hydrography and oxygen along the continental margin of Angola and Namibia were successfully recovered and redeployed. For the first time ever, velocity data describing the variability of the Angola Current and eastern boundary coastal waves off Angola is now available. Seven high-resolution hydrographic and microstructure sections that included oxygen and nutrient measurements across selected international repeat-lines in the eastern boundary current system were successfully completed, advancing the understanding of seasonal and interannual variability of hydrography, mixed-layer properties and diapycnal heat flux. At three of these sections, autonomous measurement platforms (gliders) with microstructure probes were deployed, sampling the sections at very high resolution for a period of up to four weeks. A high-resolution transatlantic hydrographic section was successfully completed using an underway sampling system. The observational program was complemented by measurements of climate-sensitive trace gas concentrations (CO_2, N_2O, CH_4 and CO_2 isotopes) and measurements of the size distribution of aerosols.

Zusammenfassung

Auf dem Fahrtabschnitt M120 wurde ein physikalisches Messprogramm mit einer biogeochemischen Komponente im Auftriebsgebiet vor Angola und Namibia durchgeführt. Das Messprogramm war ein integraler Bestandteil des EU Projektes PREFACE ("Enhancing prediction of tropical Atlantic climate and its impacts", 11/2013-11/2017) und des BMBF-Verbundvorhabens SACUS ("Southwest African Coastal Upwelling System and Benguela Niños"). Hauptziele der Untersuchungen waren (1) die Bestimmung der Variabilität des Transports der Randstromzirkulation, der Wassermassen sowie die Ausbreitung von Küstenrandwellen im Auftriebsgebiet; (2) die Quantifizierung der physikalischen Prozesse, die die Wärme- und Süßwasserbilanz der Deckschicht in dem östlichen Auftriebsgebiet bestimmen, einschließlich Wärmeverluste durch turbulente Vermischungsprozesse; und (3) die Bestimmung der Variabilität von Wassermassen entlang eines transatlantischen Schnittes auf 12°S. Insgesamt wurden neun Verankerungen mit Instrumenten zur Beobachtung von Strömungen, der Hydrographie und des Sauerstoffgehalts in dem Randstromsystem vor Angola und Namibia erfolgreich geborgen und wieder ausgelegt. Zum ersten Mal konnten dort Strömungszeitserien für die Beschreibung der Variabilität des Angolastroms und der Schelfrandwellen gewonnen werden. Sieben hochauflösende hydrographische Schnitte mit Mikrostruktur-, Sauerstoff- und Nährstoffmessungen wurden erfolgreich aufgenommen. Zusammen mit historischen Daten erlaubt der Datensatz ein verbessertes quantitatives Verständnis der saisonalen und zwischenjährlichen Variabilität der Hydrographie, einschließlich der Deckschichteigenschaften und des diapyknischen Wärmeflusses. Auf drei dieser Schnitte wurden autonome Messplattformen (Gleiter) mit Mikrostruktursensoren eingesetzt, die räumlich und zeitlich hochaufgelöste Datensätze über einen Zeitraum von bis zu 4 Wochen aufzeichneten. Ein transatlantischer hydrographischer Schnitt wurde mit einem System für Messungen vom fahrenden Schiff erfolgreich aufgezeichnet. Das Beobachtungsprogramm wurde durch

Messungen der Konzentrationen von klimasensitiven Gasen (CO_2, N_2O, CH_4 und CO_2 Isotope) und Messungen der Größenverteilung von Aerosolen vervollständigt.

2 Participants

No.	Name	Function	Institution
1	Dengler, Marcus Dr.	Chief Scientist	GEOMAR
2	Begler, Christian	Moorings, PIES, Glider, CTD	GEOMAR
3	Beier, Sebastian	Moorings, MSS	IOW
4	Boomers, Jonas	Air-sea fluxes, CTD-watch	GEOMAR
5	Cordes, Florian	Nutrients, Trace gases	IOW
6	Dippe, Tina	Salinometer, CTD-watch	GEOMAR
7	Francisco, José Amaro	Observer Angola, CTD-watch	INIP
8	Glockzin, Michael	Trace gases	IOW
9	Heene, Toralf	Moorings, MSS, CTD	IOW
10	Heitmann-Bacza, Carola	Meteorology	DWD
11	Junker, Tim, Dr.	Mooring, MSS	IOW
12	Kanga, Pedro Artur	ADCP, CTD-watch	INIP
13	Klenz, Thilo	U-CTD, MSS, Glider, CTD-watch	GEOMAR
14	Kopte, Robert	CTD, ADCP, Glider	GEOMAR
15	Logemann, Gerd	Aerosols	MPI-HH
16	Lüdke, Jan	LADCP, Glider, CTD-watch	GEOMAR
17	Mohrholz, Volker, Dr.	Senior Scientist, Moorings, MSS	IOW
18	Nielsen, Martina	CTD, Moorings, Micro-Cats	GEOMAR
19	Nielsen, Soren	Glider, CTD-watch	UCPH
20	Ostrowski, Marek, Dr.	Multibeam Echosounder, ADCP,	IMR
21	Pillar, Helen	Air-sea fluxes, CTD watch	UCPH
22	Raeke, Andreas	Meteorology	DWD
23	Seemann, Ann Katrin	O_2, CTD-watch	GEOMAR
24	Werner, Jan	Trace gases, Nutrients	IOW

GEOMAR GEOMAR Helmholtz-Zentrum für Ozeanforschung Kiel, Düsternbrooker Weg 20, 24105 Kiel, German, http://www.geomar.de/

DWD Deutscher Wetterdienst, Seeschifffahrtsberatung, Bernhard-Nocht-Straße 76, 20359 Hamburg, Germany, http://www.dwd.de/

IMR Institute of Marine Research, Department Oceanography, Nordnesgaten 50, 5817 Bergen, Norway, http://www.imr.no/en

INIP Instituto National de Investigação Pesqueira, Rua Mortala Mohamed, Ilha do Cabo, PO Box 260, Luanda, Angola, http://preface.b.uib.no/about/project-partners/inip/

IOW Leibniz-Institut für Ostseeforschung Warnemünde, Seestraße 15, 18119 Rostock, Germany http://www.io-warnemuende.de/

MPI-HH Max-Planck-Institut für Meteorologie, Bundesstraße 53, 20146 Hamburg, Germany, http://www.mpimet.mpg.de/

UCPH Niels Bohr Institutet, Kobenhavns Universitet, Blegdamsvej 17, 2100 København, Denmark, http://www.nbi.ku.dk/

3 Research Program

METEOR cruise M120 was a joint effort of the cooperative project SACUS „Southwest African Coastal Upwelling System and Benguela Niños“ funded by the German Ministry for Education and Research and the EU funded collaborative project PREFACE „Enhancing prediction of tropical Atlantic climate and its impacts“. The research objectives within the SACUS project aim at advancing our understanding of the physical mechanisms of regional climate variability and change and its consequences for the ocean’s biogeochemistry, hypoxia and marine ecosystems in the eastern upwelling region of the South Atlantic. Research within PREFACE focuses on a better understanding of the tropical Atlantic climate system, improved simulation and prediction of tropical Atlantic climate on seasonal and longer time scales and quantification of climate change impacts, including fish stock changes in the eastern upwelling regions of the tropical Atlantic.

M120 contributed to the projects‘ research goals by investigating the variability of eastern boundary current transport, water mass variability, and the propagation of coastal waves in the eastern upwelling regions of the South Atlantic (Fig. 3.1). Additionally, the cruise focused on a quantitative understanding of the physical processes controlling the mixed-layer heat and freshwater budgets. The main tasks of the physical-biogeochemical work program were to recover and redeploy mooring arrays along the continental slope and the shelf of Angola and Namibia and to conduct high-resolution hydrographic and microstructure surveys along several selected sections the eastern boundary current systems (Fig. 3.2). While the moored time series of currents, hydrography and oxygen will allow a description of the variability of the boundary current circulation and water masses, the hydrographic sections, METEORs’ meteorological measurements and the autonomous measurements will contribute to determining seasonal and interannual variability of the mixed layer heat and fresh water budgets.

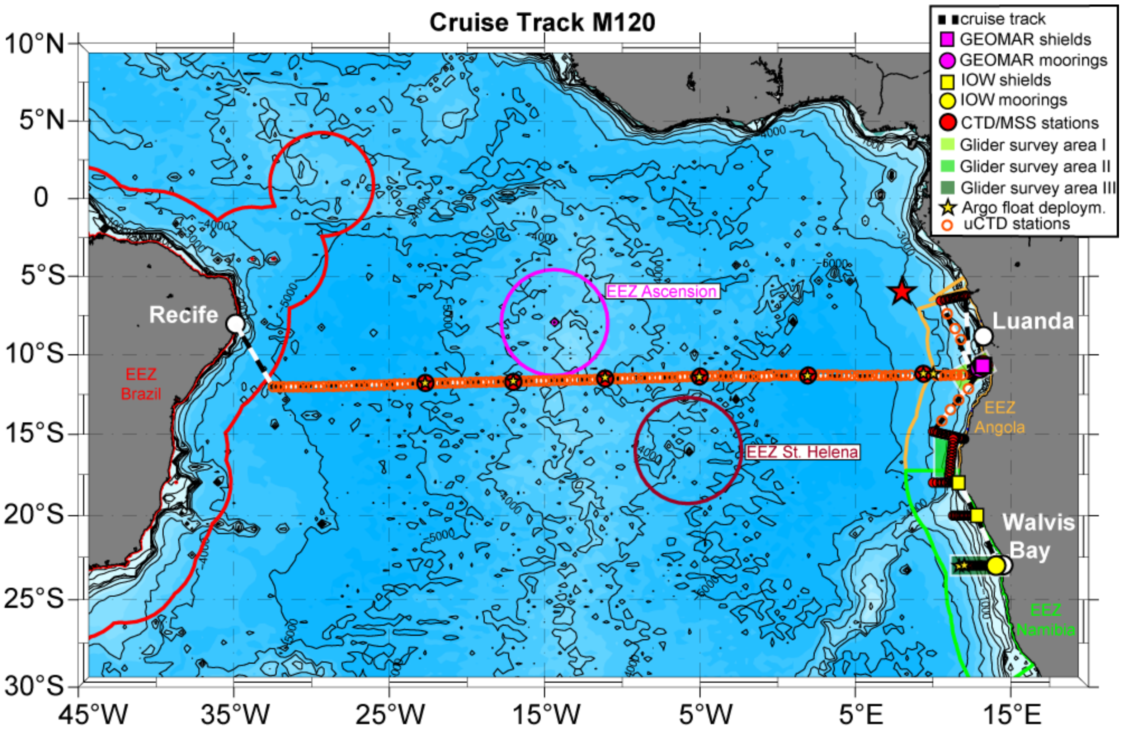

Fig. 3.1: Bathymetric map with ship track of R/V METEOR cruise M120 including locations of conductivity, temperature, depth (CTD) and oxygen and microstructure (CTD/MSS) stations, mooring and bottom shield recoveries and redeployments, glider survey areas, Argo float deployments and underway-CTD (uCTD) profiles. Territorial waters of different countries are marked with coloured solid lines.

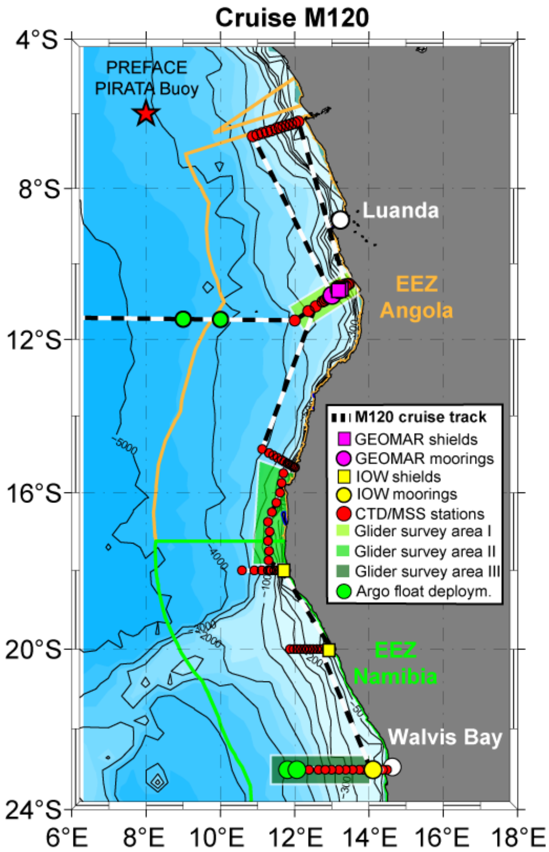

Fig. 3.2: Detailed bathymetric map and M120 cruise track of the Angolan and Namibian survey area. The map includes locations of CTD/MSS stations, mooring and bottom shield recoveries and redeployments, as well as glider survey areas and Argo float deployments. Territorial waters of Angola and Namibia are marked with beige and green solid lines, respectively.

4 Narrative of the Cruise

Prior to R/V METEOR cruise M120, most of the participating scientists joined the IVth Seminar of the Bilateral Cooperation DOCEAN – GEOMAR held at the Federal University of Pernambuco in Recife on October 14, 2015, a seminar series that was initiated during a visit of R/V METEOR in Recife in 2002. R/V METEOR left the port of Recife on Saturday, October 17 at 7:30 local time. Due to necessary repairs of METEOR's central hydraulic system on short notice, the departure originally scheduled for October 16 was delayed by one day. On October 18 at 12:00 UTC, just after leaving the exclusive economic zone of Brazil (Fig. 3.1), the observational program started with collecting underway profiles of conductivity, temperature, and depth (uCTD) on a transect across the Atlantic along 12°S. All underway sampling systems, including the two METEOR's ocean surveyor ADCPs measuring upper ocean currents and continuous sampling of surface water trace gas concentrations started data recording at this position. The transatlantic uCTD section was completed 10 days and 4 hour later at 11.5°S, 11.7°E. The hourly uCTD sampling rate resulted in 230 hydrographic profiles. Additionally, six Argo floats provided by the Bundesamt für Schifffahrt und Hydrographie were released and five conductivity, temperature, depth and oxygen (CTD/O_2) profiles to a water depth of 2000 m were collected on the transect.

R/V METEOR entered Angolan territorial waters on October 28 at 04:00 UTC (Fig. 3.2). For the next 4 days, works focused on retrieving and redeploying a mooring array and sampling of the water column along a cross-slope section at 11°S (Fig. 3.2). During METEOR cruise M98 in July 2013, almost 2 ½ years prior to M120, two moorings, two bottom shields and a bottom pressure sensor had been deployed along the 11°S section. Due to several different circumstances, the moored equipment could not be serviced as scheduled in autumn 2014. We were thus relieved to be able to recover most of our instruments after the unexpectedly long deployment period. The two most important components of the array were recovered, a bottom shield instrumented with an acoustic Doppler current profiler (ADCP) deployed at 500 m and a mooring deployed at 1200 m depth that included a long-ranger ADCP as well as the bottom pressure sensor (see section 7.2 for details of the mooring instrumentation). No response was received from the releasers of the not-recovered mooring and bottom shield deployed at 300 m and 200 m depth, respectively. In an attempt to recover the 300 m mooring (KPO 1105), a dredging operation was prepared in the early morning of October 30 by deploying a wire with 8 attached grapnels in a semi-circle around the mooring position and subsequently heaving it back on board. Since the mooring location was known very precisely, such dredging should cut the thin wire and let the mooring float up to the surface. However, the operation was unsuccessful leading to the conclusion that it was no longer in its place. Likewise, attempts to locate the unrecovered bottom shield deployed at 200 m (KPO 1104) by acoustic methods failed. The fate of the bottom shield remains unknown. In the afternoon of October 30, a short term mooring (KPO 1168) mooring was deployed. The two ADCPs attached to the mooring were configured to sample in a very high-resolution mode to record the full internal wave spectrum.

Water column sampling along the 11°S section carried out between the mooring operations included collecting CTD/O_2 profiles (Fig. 3.2) as well as lowered ADCP profiles (lADCP), a system of current meters attached to the rosette frame. Water samples from the Niskin bottles were analyzed for concentrations of salinity, oxygen and nutrients (NO_3^-, NO_2^-, PO_4^{3+}, NH_4^+) and samples for the analysis of trace gases (N_2O and CH_4) were prepared for transportation to Germany. Furthermore, turbulence measurements using a microstructure probe (MSS) were taken prior or after each CTD/O_2 station. Usually, three profiles in deeper waters (>100 m) and five microstructure profiles in shallower waters (<100 m) were collected. Sampling of shipboard velocity profiles by the vessel mounted Ocean Surveyor ADCPs was continued throughout the cruise. Shortly before leaving the 11°S section, a glider with a turbulence probe attached was deployed to continue sampling data along the 11°S section for the following month. The glider was retrieved on the subsequent METEOR cruise M121.

After completing the measurement program at the 11°S section in the evening of October 31, we headed north to work on a cross-slope section at 6°S (Fig. 3.2). Unfortunately, a member of the crew was seriously injured and METEOR's physician determined that he needed to be hospitalized. Captain Hammacher decided to change METEOR's course in the morning of November 1 to bring the injured crew member to Luanda, the capital of Angola. Despite the unavailability of Angola's sea rescue service, but with the help of the Angolan observer the crew member was brought to a hospital in the late afternoon. METEOR returned to the original cruise track 18 hours later and arrived at the 6°S section at 9:45 on November 2. Sampling along the 6°S section included 13 CTD/O_2 and lADCP profiles as well as 13 MSS stations. Additionally, water samples from the CTD rosette were analyzed for concentrations of salinity, oxygen, nutrients and trace gas concentrations. This section as well as the 11°S and 15°S sections (Fig. 3.2) are repetitions of hydrographic sections within the Nansen Programme of the Food and Agriculture Organization (FAO) of the United Nations that are regularly occupied by R/V FRIDTJOF NANSEN in March/April and June/July. These measurement campaigns are carried out in cooperation with our Angolan colleagues and partners within EU-PREFACE project from the Instituto National de Investigação Pesqueira (INIP). Our contribution was to sample the section in austral spring to identify seasonal and interannual variability of water masses and currents.

On November 3 at 08:00, the 6°S section was completed and METEOR took a southward course to the mooring deployment positions at 11°S. During the transit, uCTD profiles were taken. The two mooring (KPO 1151 and KPO 1153), the bottom shield (KPO 1152) and a pressure inverted echo sounder (KPO 1155) were successfully deployed along the 11°S section on the following day. Both of the mooring deployments used the rear gallows and each were accomplished in only one hour. For the deployment of the bottom shield, winch 2 instead of winch 11 was used. This turned out to be a good choice because the release of the bottom shield 1 m above the bottom was clearly visible in the wire tension data of winch 2. Finally, the short term mooring KPO 1168 was recovered after 5 days of deployment. Due to the professionalism of METEOR's deck crew and the technical staff, we were able to successfully complete 5 mooring operations in a single day. After collecting two more CTD profiles on the 11°S section, METEOR continued southwards to the 15°S section just after midnight, again collecting uCTD profiles during transit (Fig. 3.2). Along the 15°S section, 12 CTD/O_2 and lADCP profiles were taken and 12 MSS stations were conducted. The section was completed on November 7 at 10:00.

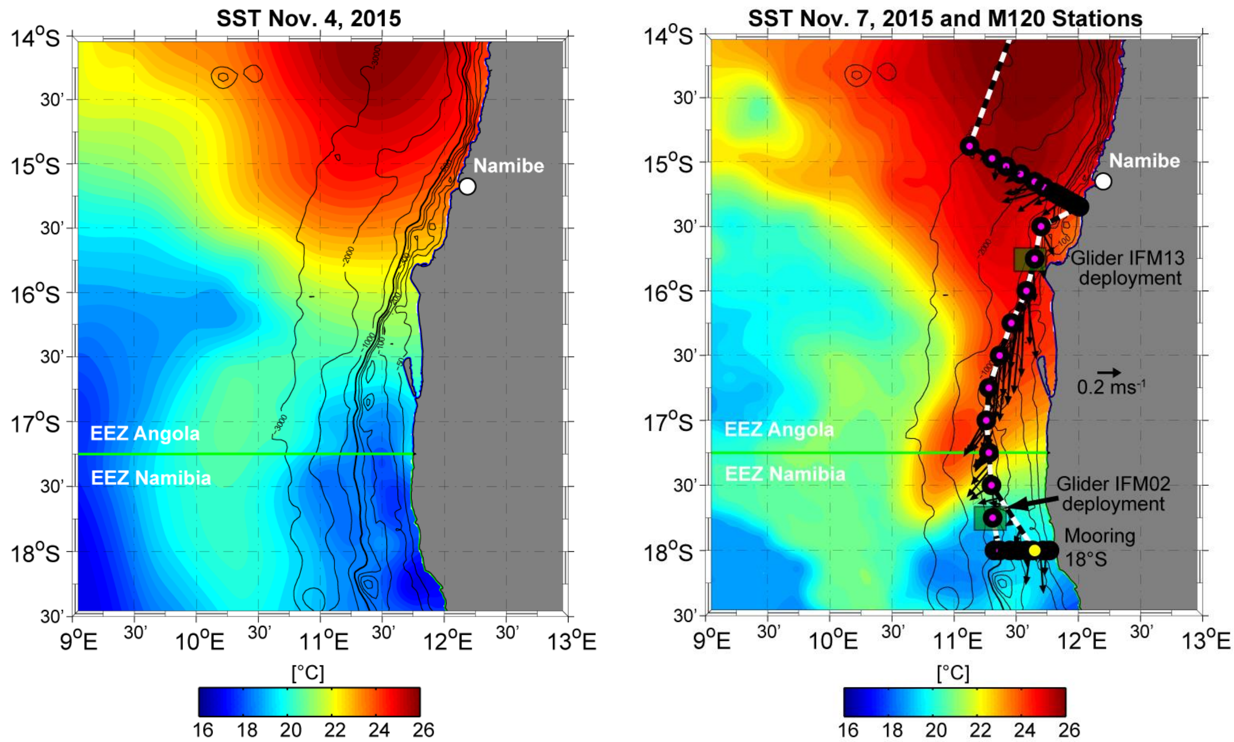

Fig. 4.1: Sea surface temperature from November 4 (left panel) and November 7, 2015 (right panel) from satellite observations. METEOR's cruise track (black-while dashed line), CTD/O_2 stations (purple circles), the position of the 18°S mooring (yellow circle) as well as near-surface currents from the vessel-mounted ocean surveyor (black arrows) are indicated in the right hand panel. The southward displacement of the front resulted in a sea surface temperature increase of more than 5°C in the region of the continental slope and shelf from 15°30'S to 17°30'S.

Between 15°S and 18°S, the Angola-Benguela frontal zone is located (Fig. 4.1). It separates warm near-surface waters to the north from cold near-surface waters to the south. Temperature difference across the front typically ranges from 5°C to 8°C. A CTD/O2 and shipboard ADCP section complemented with uCTD profiles along the 500 m isobaths was collected to advance understanding of the frontal dynamics. Water samples from the CTD rosette were analyzed for concentrations of salinity, oxygen and nutrients and samples for the analysis of trace gases were prepared. During the section occupation, elevated southward flow of more than 20 cm/s in the upper 50 m of the water column resulted in a fascinating southward displacement of warm water that was also reflected in satellite imaginary of sea surface temperature (Fig. 4.1). A strengthening of the trade winds accompanied the southward displacement of the front. To advance our understanding of the variability of the front and associated ocean-atmosphere interactions and ocean feedback processes in the frontal region, two gliders were deployed that sampled the frontal region along meridional transects in the following month until recovery during the follow-up cruise M121.

In the afternoon of November 8, R/V METEOR reached the 18°S section and a bottom shield moored at 125 m depth on the shelf (Fig. 4.1) was successfully recovered. Although the release of the bottom shield malfunctioned, a catch line that was attached to the shield was dredged on the second try using a grapnel attached to the end of the ship's wire. A mooring configured for high-frequency sampling was subsequently deployed at the same position. Altogether, 16 CTD/O_2 and lADCP profiles and the same number of MSS stations were taken along a zonal transect at 18°S. Water samples were again analyzed for concentrations of salinity, oxygen and nutrients, while water samples for trace gases analysis were prepared for transport. At noon on November 10, the mooring sampling at high-frequency was recovered and the bottom shield was redeployed at the same position from where it was retrieved. At 14:00 that day, METEOR headed further southward to 20°S.

CTD/O_2 sampling at the zonal 20°S section (Fig. 3.2) was started at 04:00 on November 11. Works on the section were identical to work performed at 18°S. CTD/O2 and MSS stations were taken while moving westward along the section. The position of a bottom shield was reached just after 09:00. This time, the bottom shield was successfully released. Again, a mooring sampling at high-frequency was deployed for the period of bottom shield servicing. The 20°S and 23°S sections are surveyed on a regular basis by our Namibian colleagues and partners within EU-PREFACE project from the National Marine Information and Research Center (NatMIRC) in Swakopmund, Namibia. While heading west along 20°S, 20 CTD/O_2 and 20 MSS stations were sampled. The bottom shield was redeployed and the mooring sampling at high-frequency was recovered in the morning of November 13.

In the morning of November 14, sampling along our final section at 23°S (Fig. 3.2) commenced. Due to strong winds reaching 8 Beaufort and swell of more than 3.5 m, the recovery of a mooring and a sediment trap as well as the scheduled deployment of a glider had to be postponed. However, CTD/O_2 and MSS stations could still be carried out. Heading west, the 23°S section was sampled and two ARGO floats were released until winds and swell weakened in the evening of November 15. METEOR then headed back inshore to retrieve two moorings deployed at 130 m water depth in the early morning of November 16. After successful recovery of both moorings, a glider with an attached microstructure probe was deployed in a water depth of 300 m. Recovery of the glider was planned during the follow-up cruise M121. The CTD/O_2 and MSS section work was continued until the morning of November 17. Redeployment of the two moorings on the shelf at 23°W started at 10:30 that day and finished shortly after midday. R/V METEOR then sailed to the port of Walvis Bay arriving just after 17:00. Unfortunately, due to the unavailability of a berth, METEOR had to anchor in proximity of the port. After packing was completed, the scientific crew was picked up by a shuttle at noon on November 18.

5 Preliminary Results

In the following, a detailed account of the types of observations, methods and instruments used as well as some of the early results are presented.

5.1 Hydrographic observations

(Gerd Krahmann, Volker Mohrholz, Robert Kopte, Thilo Klenz, Ann Katrin Seemann, Tina Dippe, Marcus Dengler)

5.1.1 CTD system, oxygen measurements, and calibration

During M120 a total number of 114 CTD/O_2 profiles were collected in most cases to full ocean depth. Positions and profiling depth of the casts are detailed in the station list in section 7.1. During the whole cruise the GEOMAR SBE#3, a Seabird Electronics (SBE) 9plus underwater unit, was used. It was attached to a GO4 rosette frame. The SBE3 was equipped with one Digiquartz pressure sensor (s/n 82991) and double sensor packages for temperature (T), conductivity (C) and oxygen (O) (primary set: T_1 = s/n 2120, C_1 = s/n 3425, O_1 = s/n 2600; secondary set: T_2 = s/n 4051, C_2 = s/n 3959, O_2 = s/n 2686). Additionally, fluorescence and turbidity sensors (Wetlabs) were attached to the SBE3 and a sensor measuring the intensity of photosynthetically active radiation (PAR) was attached to the top of the rosette frame during CTD/O_2 casts shallower than 2000 m depth. Finally, a lowered ADCP (lADCP) and 22 10-liter bottles were attached to the rosette frame. All sensors worked well throughout the cruise. Data acquisition was done using Seabird Seasave software version 7.23k.

For calibration of the conductivity and oxygen sensors, conductivity values were determined from 261 water samples using a Guildline Autosal salinometer (AS) and oxygen concentrations were determined from 393 water samples using Winkler titration. Throughout the cruise, conductivity values from the water samples were analyzed using the GEOMAR salinometer AS 7 (Model Guideline 8400 B). During the 13 days when the instrument was in use, only small adjustments to the standardization potentiometer were necessary and subsequent sub-standards determinations performed several times each day indicated an adequate stability of the instrument. For Winkler titration measurements, the same measurement setup and titration procedures as during M119 were used. For details, the reader is referred to section 5.2.1 in the METEOR M119 cruise report (Brandt et al., 2016).

The conductivity and oxygen sensors were calibrated using linear dependences of pressure, temperature and conductivity from the salinometer and Winkler titration derived values, respectively. Additionally, oxygen calibration accounted for second order dependencies in pressure. The misfit, taken here as the root-mean square of the differences between calibrated CTD/O_2 sample values and the respective water samples, was 0.00020 S/m and 0.00021 S/m for the C1 sensor and C2 sensor, respectively, and 1.31 µmol/kg and 1.17 µmol/kg for the primary and secondary oxygen sensors, respectively. In terms of salinity, the misfit yields 0.00191 psu for C1 and 0.00208 psu for C2. For each fit, the 33% most deviating water samples values were removed to exclude biases by bad samples. For the final data set that will also be publically available, the secondary sensor set was used for all CTD/O_2 stations except for profiles 62, 96, and 97. The pump of the second sensor set was blocked during those casts and thus the first sensor set was used. Data from the fluorescence and turbidity sensors and the PAR sensor were not calibrated.

5.1.2 Underway-CTD measurements and calibration

A total of 265 underway conductivity-temperature-depth (uCTD) profiles were taken along the transatlantic transect at 11°S and during transits from 6°S to 11°S and from 15°S to 18°S (Fig. 3.1). The acquired data allows determining water mass variability across the Atlantic (Fig. 5.1) and variability of the mixed layer properties. Additionally, uCTD profiles collected along 15°S to 18°S were performed in between CTD stations to better resolve the Angola-Benguela front. uCTD profiles were sampled every hour to a mean profile depth of about 400 m while steaming at full speed of the vessel. Two different probes (s/n 0238 and 0239) were used. On October 27th at 06:00 UTC, close to the end of the transatlantic transect, a probe (s/n 0239) was lost because the line tore after starting the uCTD winch to recover the probe. The line was renewed and the remaining probe was used for the last 32 profiles.

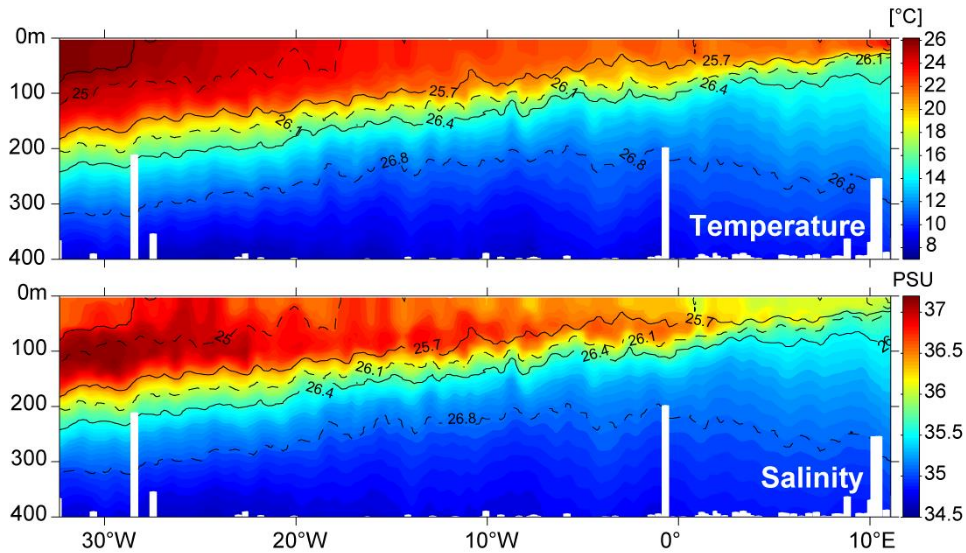

Fig. 5.1: Temperature and salinity distribution from the uCTD measurements along the 12°S transect. Black solid and dashed lines indicate isopycnals in kg m^{-3}.

For calibration of the uCTD sensors, uCTD profiles were collected just before and shortly after CTD stations. Additionally, the probes were attached to the CTD/O_2 rosette to identify possible pressure offsets. Ongoing calibration includes thermal lag calculation, pressure offsets from CTD/O_2 comparison and temporal sensor drifts determined from nearby CTD/O_2 profiles and from surface temperature and salinity measurements from the thermosalinograph.

5.1.3 Thermosalinograph calibration

Sea surface temperature and sea surface salinity were continuously measured by METEOR's new dual thermosalinograph. The new system consists of two devices, one with an inlet at the starboard side (TSG1) and the second with an inlet at the portside (TSG2). Both systems worked well throughout the cruise.

The two external temperature sensors, $T1_{sec}$ from TSG1 and $T2_{sec}$ from TSG2, and both conductivity sensors (S1, S2) were calibrated against the 5 dbar values from the 114 CTD/O_2 profiles taken during the cruise. A sensor drift for the external temperature sensors relative to the CTD values was not significant. However, when directly comparing $T1_{sec}$ and $T2_{sec}$, a small drift of $5x10^{-3}$°C between October 23 and November 18 was suggested. The mean offsets for T1sec and T2sec relative to the 5 dbar values of the CTD/O_2 measurements were +0.0005°C and -0.0002°C, respectively. Estimated root mean square uncertainties for $T1_{sec}$ and $T2_{sec}$ were ±0.0096°C and ±0.00051°C.

In contrary, sensor drifts for both conductivity sensors relative to the 5 dbar values from the 114 CTD/O_2 profiles could be identified (Fig. 5.2). Although sensor S1 did not show a drift relative to the 5 dbar CTD/O_2 values during the first 18 days of the cruise, a drift of about 0.0179 psu per day was identified after November 3 (Fig. 5.2). Relative to the same 5 dbar CTD/O2 reference, sensor S2 showed a weak drift from the first day of the cruise until day 20, followed by an elevated linear drift of 0.0286 per day until day 28. On that day, the differences of the S2 and CTD/O_2 salinities suddenly vanished, but then increased approximately linearly again (Fig. 5.2). The reason for the different behavior of the two conductivity sensors could not be identified. No drift could be detected for the internal temperature sensors $T1_{prim}$ and $T2_{prim}$ that are used to calculate salinity from the measured conductivities. A possible explanation may be that the conductivity cells get blocked over time and need to be cleaned more often. Certainly, more dedicated investigations of this problem are required.

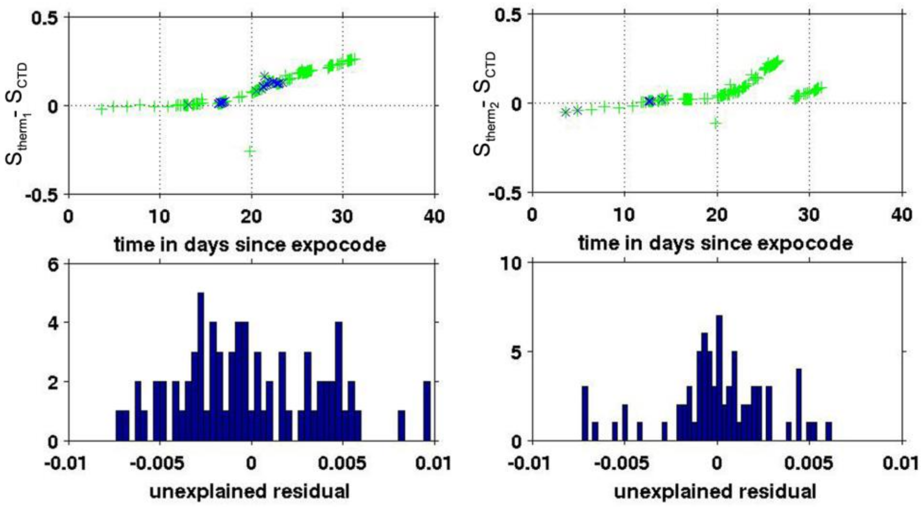

Fig. 5.2: Differences between salinities measured by conductivity sensor 1 of the thermosalinograph system and salinities measured by the CTD/O_2 at 5 dbar against time in days since the start of the cruise (upper left panel). Upper right panel shows salinity differences of the thermosalinograph conductivity sensor 2 and the 5 dbar CTD/O_2 salinity measurements against time (days). Lower panels present the histogram of salinity differences of the same sensors and the 5 dbar CTD/O2 salinity values after calibration of the respective thermosalinograph conductivity sensors using linear trend corrections.

5.2 Current observations

5.2.1 Vessel mounted ADCP

(Jan Lüdke, Robert Kopte, Marcus Dengler)

Upper-ocean velocities along the cruise track were recorded continuously by the two vessel mounted Ocean Surveyor systems of R/V METEOR. Both systems worked well. Data recording was discontinued only during periods of acoustic communications with releasers during mooring and bottom shield recoveries. The 38 kHz RDI Ocean Surveyor (OS38) system was operated in narrowband mode with 32 m bins and a blanking distance of 16 m while 55 bins were recorded. Although originally planned to be operated in broad-brand mode, the 75 kHz RDI Ocean Surveyor (OS75) was changed to narrow-band mode operation after the first day of data recording due to low abundance of backscatters in the water column. This configuration that included 100 recorded bins of 8 m length and a blanking distance of 4 m was used throughout the cruise. The measurement range of the OS75 was 600 m for most of the cruise while it was somewhat lower in the western tropical South Atlantic due to the reduced backscatter abundance. The OS38 recorded valuable data to about 1000 m depth during the whole cruise.

Data post-processing carried out for both systems included water track calibration of the misalignment angle and the amplitude of the Ocean Surveyor signal (Tab. 5.1). The results of the OS75 misalignment angle calibration agreed very well with the results obtained during the previous cruise M119, where an angle of 1.09° was determined. As the OS75 is built into the ship's hull, an agreement is to be expected. Nevertheless, a difference in calibration of the misalignment angle between the two cruises of only 0.07° indicates the stability of the ocean surveyor and navigational devices as well as the accuracy of the post-processing method.

Tab. 5.1 Results of the post-processing of the Ocean Surveyor data.

OS	Mode	Misalignment angle ± Standard deviation	Amplitude factor ± Standard deviation
75	NB	-1.0238° ± 0.6182°	1.0035 ± 0.0105
38	NB	-0.2940° ± 0.5735°	1.0050 ± 0.0082

Of particular interest were the shipboard velocity observations across the Angola-Benguela Front along the 11°E section (Fig. 5.3). Elevated southward near-surface velocities observed along this section caused the southward displacement of the front during our survey (see Fig. 4.1). Southward velocities in the deeper water column as observed across the front (Fig. 5.3) may be associated with the Angola Current that strengthens in this region (e.g. Xu et al., 2014).

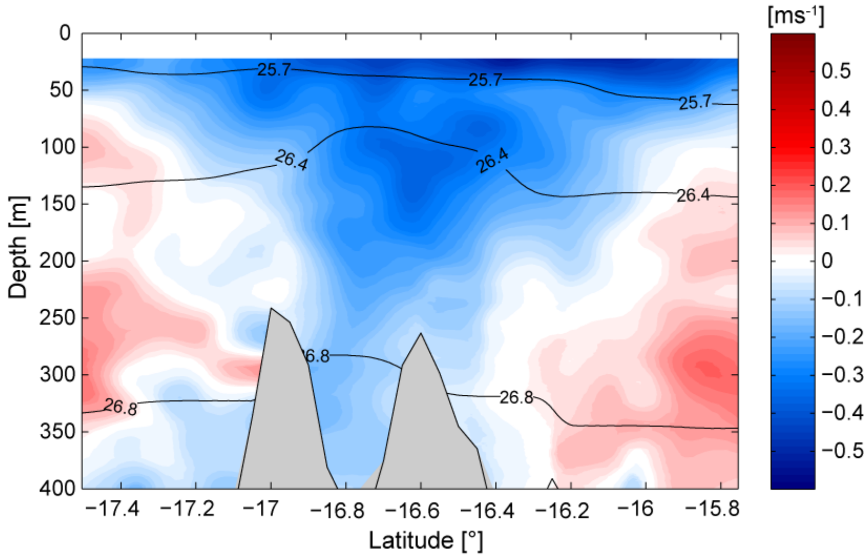

Fig. 5.3: Meridional velocity along the meridional 11°E section measured by the OS75 system. Grey shading marks bottom topography and black lines show isopycnals determined from the CTD stations (for CTD positions see Fig. 3.2).

5.2.2 Lowered ADCP measurements

(Jan Lüdke)

Lowered ADCP measurements were performed to observe near-bottom currents during CTD stations. Due to bottom-reflection of the acoustic signal from the ship-board ADCP, the last 15% of the water column velocities from this instrument are erroneous. The lADCP profiles can fill most of this gap. Thus, an lADCP system was mounted to the rosette frame of the CTD. It consisted of an upward and a downward looking 300 kHz ADCP, S/N 11436 and S/N 20508, respectively. The downward looking ADCP was operated as master. The system performed well throughout the cruise, although there was some weak interference with the altimeter of the CTD. No data was recorded during CTD profile 15 due to an operator handling error. Furthermore, no lADCP velocity data is available for CTD profile 96, because of water depth was too low (39 m) for adequate data processing. Post-processing of the lADCP data was done using the GEOMAR lADCP software in Version 10.21. Upper ocean velocities were constrained by OS75 velocity data and additional input of navigational data as well as profiles of temperature, salinity and pressure taken from the processed CTD data.

5.3 Mooring operations

(Marcus Dengler, Volker Mohrholz)

5.3.1 Mooring array in Angolan waters at 11°S

During METEOR cruise M98 in July 2013, nearly 2 ½ years before M120, two moorings, two bottom shields and a bottom pressure sensor were deployed perpendicular to the coastline at 11°S along the Angolan continental slope. The moorings and bottom shields were equipped with ADCPs to observe the variability of the eastern boundary circulation and to determine intraseasonal to interannual variability of the transport of the Angola Current. Additionally, a mooring deployed at 450 m carried oxygen, temperature and salinity logger at 4 different depths to analyze water mass variability. Due to several different circumstances, the moored equipment could not be serviced as scheduled in autumn 2014.

During M120, only one bottom shield, the mooring deployed at 1200 m depth and the bottom pressure sensor mooring could be recovered. No acoustic response was received from the releasers of the mooring deployed at 450 m depth and from the release of a bottom shield deployed at 200 m depth. As detailed in the narrative of the cruise (section 4), a dredging operation was carried out in an attempt to recover the 450 m mooring (KPO 1105). However, the operation was unsuccessful and it was concluded that the mooring was no longer in its place. Likewise, attempts to locate the unrecovered bottom shield deployed at 200 m (KPO 1104) using the multi-beam echo sounder failed. The fate of the bottom shield remains unknown. However, the bottom shield recovered from 500 m depth showed strong corrosion of bolts and other parts of the shield. Due to the way the bottom shield was constructed, strong corrosion could lead to a premature release of the shield. All instruments attached to the recovered moorings and the bottom shield worked well throughout the deployment period. Detailed information on the moorings and on the time series of the attached instruments is given in table 7.2.1.

Despite the limited recovery, two mooring (KPO 1151 and KPO 1153), a bottom shield (KPO 1152) and two pressure inverted echo sounder were successfully deployed along the 11°S section in Angolan waters. Additionally, a short term mooring (KPO 1168) mooring was deployed and recovered during the cruise. The two ADCPs attached to the short-term mooring were configured to sample in a very high-resolution mode to fully record internal wave activity in between the recovery and redeployment period of the array. Detailed information of the deployed moorings is listed in table 7.2.1.

5.3.2 Mooring operations on the Namibian shelf

IOW operates an array of three long-term moorings along the northern Namibian shelf at a water depth of about 130 m. The major aim of that array is to evaluate the variability of eastern boundary current transport, variability in the advection of anomalous water masses along the eastern boundary and wave propagation along the southwest African coastal wave guide. The two northernmost moorings (LTKC, LTTB) are equipped with an upward looking ADCP mounted in a trawl resistant bottom frame. Additionally, a SeaBird 37 MicroCat thermosalinometer and a PME MiniDOT oxygen sensor are mounted. The southernmost mooring (LTMB) is a water-column mooring equipped with thermosalinometers, oxygen optodes, temperature and pressure recorders and an upward looking ADCP. At the same position as the LTMB mooring, a sediment trap mooring (STMB) is operated by the University of Hamburg. All mooring were maintained and redeployed by R/V Mirabilis in January 2015. During M120, these moorings were successfully recovered, maintained and again redeployed. Details of the deployment periods are listed in table 7.2.2. The next maintenance is scheduled for May 2016 with R/V Mirabilis.

During the period between mooring recovery and redeployment, high-resolution moorings were deployed at about the same position as the long-term moorings (see table 7.2.3). The main purpose of these high resolution moorings was to obtain hydrographic data from the lower and upper boundary layer with a high temporal resolution on the order of a few seconds. The data is appropriate for detecting internal waves and other short term processes that control the vertical mixing and resuspension of particular matter on the sea floor. Each mooring consists of two 600 kHz Workhorse ADCP. Deployments at 18°S and 20°S (HR_120_1 and HR_120_2) were designed such that one ADCP is mounted at 40 m depth looking upward and a second instrument (placed about 40 m above the bottom) is looking downward. In contrast, both ADCPs are looking upward in the 23°S deployment (HR_120_3). Additionally, all moorings were equipped with four SeaCat thermosalinometers SBE16 and three RBR TR160 temperature recorders.

5.3.3 Velocity time series from moorings on the Namibian shelf

As an example of the gathered data, Fig. 5.4 depicts the north component of current velocity at two mooring positions on the Namibian shelf. The preliminary data highlight both, the mainly barotropic character of the along shore flow and the high correlation of alongshore currents on the northern Benguela shelf. Due to the narrower shelf width the mooring at 18°S is located closer to the shelf edge, compared to the mooring at Terrace Bay. The narrow shelf is also one reason why for the enhanced velocities at 18°S compared to 20°S.

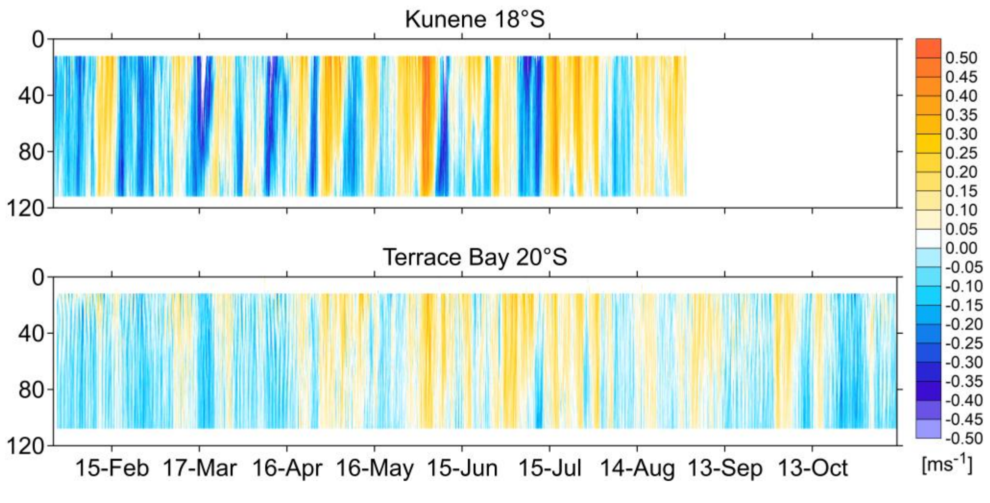

Fig 5.4: Meridional velocity measured with the long-term moorings at 18°S (top panel) and 20°S (bottom panel).

5.4 Shipboard microstructure measurements

(Volker Mohrholz, Tim Junker, Toralf Heene, Sebastian Beier)

An extensive microstructure measurement program was carried out aiming at evaluating mixed layer heat and freshwater balances along the continental margins and investigating mixing processes at the continental margins in upwelling regions.

5.4.1 Microstructure system overview

The ship-based microstructure measurements were performed using a loosely-tethered MSS 90-S (S/N 055) microstructure profiler and a power-block winch mounted at the portside of METEOR. The MSS profiler was equipped with 2 fast-responding shear sensors for turbulence measurements, a microstructure temperature sensor, standard CTD sensors for precision measurements, oxygen sensor, turbidity sensor, and an acceleration sensor. All sensors were mounted to the head of the profiler and the microstructure sensors were placed about 150 mm ahead of the other sensors. All sensors sampled at a rate of 1024 measurements per second. At each microstructure station 2 to 6 profiles were collected. The profiler was ballasted with negative buoyancy to adjust the sinking velocity to 0.6 m/s. It was operated via a power block winch from the stern of R/V METEOR. In total, 400 profiles were collected during 103 stations along the seven transects (Figs. 3.1 and 3.2, Table. 7.1).

Three different types of air foil shear sensors were used (Fig. 5.5): Standard MSS shear sensors (PNS06, type A), MSS shear sensors with an enlarged air foil tip (PNS08, type B), and MSS shear sensors with rubber sealed tip (type C). A technical focus of the measurement program was to determine the detection limit of the different sensors. A comparable performance was found for the different sensor types in environments with elevated turbulent kinetic energy (TKE) dissipation rates above 10^{-9} W kg^{-1}. At those turbulence levels, the shape of the shear spectra of all sensors nicely agreed with the shape of the universal Nasmyth spectrum (Wolk et al., 2002). Below these turbulence levels minor differences in spectral shape between the different sensor types were found. The first preliminary analysis suggests a slightly lower detection limit for sensor type C. However, the majority of measurements were performed in environments with TKE dissipation rates above 10^{-9} W kg^{-1}. Thus, the quality of the TKE dissipation measurements performed during the cruise M120 depends not on the particular used sensor type.

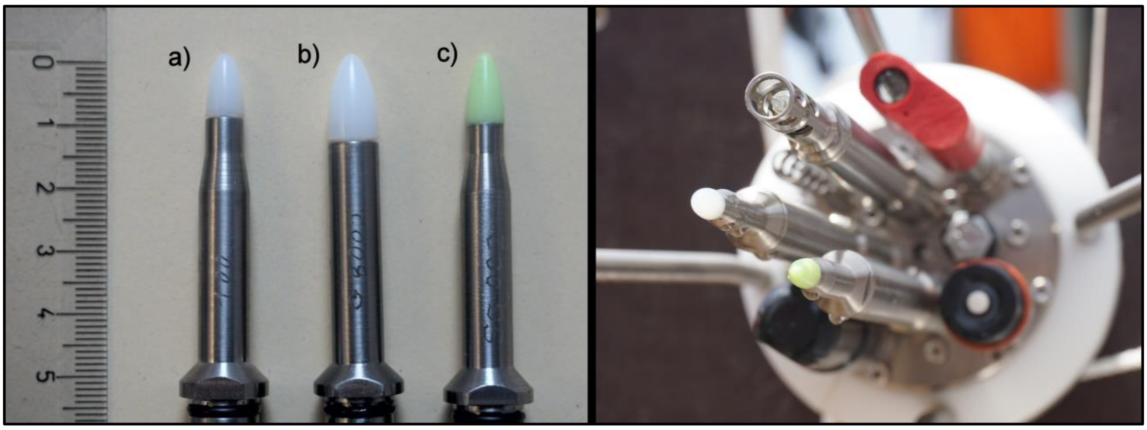

Fig. 5.5: Different types of airfoil shear sensors used during the cruise (left panel). Sensor-head of MSS profiler with mounted shear sensors of type A and C (right).

5.4.2 Microstructure observations

At all seven sections, the MSS measurements revealed elevated variability of turbulence and hydrography. During the northernmost section at 6°S, enhanced TKE dissipation rates and eddy diffusivities were observed inshore of the shelf break near the ocean floor and in the upper thermocline (Fig. 5.6). Additionally, the repeated hydrographic profiles indicated elevated high-frequency variability of vertical displacements in the thermocline and near-bottom turbidity on the shelf was enhanced (Fig. 5.6). These finding indicate elevated internal wave levels and their breaking at critical angles of topography to be the likely cause of the enhanced TKE dissipation rates and elevated eddy diffusivities at this section. Generally, the distribution of TKE dissipation rates at the other section between 11°S and 23°S showed similar features as described for the 6°S section.

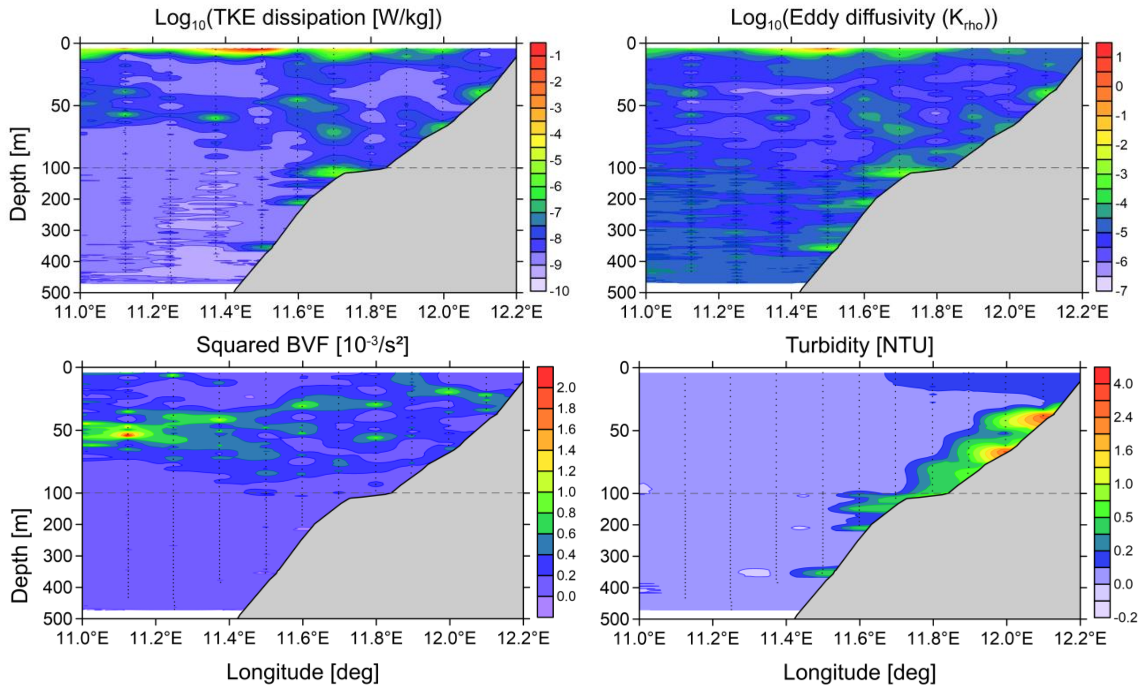

Fig. 5.6: Upper panels depict distribution of TKE dissipation rates (left) and eddy diffusivities (right) along the 6°S section just south of the Kongo river inflow. Lower panels show stratification (left) calculated from the CTD data and turbidity (right). Please note that the upper 100 m of the y-axis in all plots are stretched.

5.5 Glider operations

(Marcus Dengler, Christian Begler)

An integral component of the observational program was the deployment of gliders to sample the variability of hydrography, oxygen, turbulence, nutrients and various other parameters at high spatial resolution across Angola-Benguela front and along the 11°S and 23°S sections (Fig. 3.2) for a period of 20 to 30 days.

5.5.1 Glider configuration and missions

Altogether, four Teledyne Webb Research Slocum gliders (ifm02, ifm03, ifm09, and ifm13) were deployed during M120 and retrieved during the follow-up cruise M121. The gliders were equipped with temperature, conductivity, pressure, oxygen, chlorophyll and turbidity sensors. In addition, microstructure probes (MicroRider, manufactured by Rockland Scientific) were mounted to the gliders ifm02, ifm03 and ifm09 and an optical nitrate sensor (SUNA, manufactured by Satlantic) was mounted to glider ifm13 (Tab. 5.2). All microstructure probes carried two microstructure shear and two microstructure temperature sensors as well as fast-responding accelerometers and tilt sensors.

Glider ifm03 was deployed at 11°S on Oct. 31 and sampled the 11°S section nine times before it was retrieved on Nov. 28. On Nov. 12, the glider hit an unidentified obstacle near the surface shortly after beginning its dive during profile 313. The collision damaged the microstructure sensors mounted on the MicroRider and caused a leakage into the MicroRider's nose cone. To reduce further leakage, maximum diving depth was reduced from 1000m to 500m starting from profile 315. No microstructure data are available from ifm03 after Nov. 12. Glider ifm02 and ifm13 were deployed on Nov. 7 and 9 to sample across the Angola-Benguela front along about 11°E. Both gliders worked well throughout the deployment period and the 11°E section from 15.8°S to 17.8°S was sampled twice by each glider while running in opposite direction. Ifm09 was deployed at 23°S on Nov. 16 and recovered on Dec. 24. Ifm09 also worked well throughout the mission and collected more than 1200 CTD profiles while zonally sampling the 23°S section between 12°E and 13.5°E five times. Sampling of microstructure data was discontinued after Dec. 1 to reduce power consumption. A summary of the glider deployments and mission-specific parameters are listed in the table 5.2. Details of the missions and plots of the satellite-transmitted data can be retrieved from http://gliderweb.geomar.de/.

Tab. 5.2: Summary of glider missions.

	Ifm02	**Ifm03**	**Ifm09**	**Ifm13**
Mission	Depl23	Depl12	Depl06	Depl03
Survey area	Angola-Benguela front	11°S section	23°S section	Angola-Benguela front
Deployment date	Nov. 9, 12:00	Oct. 31st, 08:00	Nov. 16, 16:30	Nov 7, 13:30
Recovery date[1]	Nov. 24, 08:00	Nov. 28, 09:00	Dec. 24, 11:00	Nov. 25, 06:00
Sensors	p, T, S, O_2, chl-a, turbidity	p, T, S, O_2, chl-a, turbidity	p, T, S, O_2, chl-a, turbidity	p, T, S, O_2, chl-a, turbidity
Mounted probes	Microstructure	Microstructure	Microstructure	Nitrate (SUNA)
Number of profiles	454	780	1218	576
Max. depth (db)	504	1010	1013	514

[1] The glider were recovered during FS METEOR cruise M121.

5.5.2 Glider observations

The oxygen distributions across the Angola-Benguela front at 11°E (Fig. 4.1) measured by the gliders indicated elevated variability in the deeper water column in region of the frontal zone (Fig. 5.7). Previous observations had indicated a steady southward decrease of oxygen content in the upper thermocline (e.g. Mohrholtz et al., 2008; Monteiro et al., 2008). However, the high spatial resolution oxygen sections from the gliders suggest a local oxygen maximum occurring within the frontal region. The local oxygen maximum may result from an along-front advection or enhanced diapycnal oxygen fluxes from the surface due to elevated mixing in the frontal region. Both processes are currently investigated.

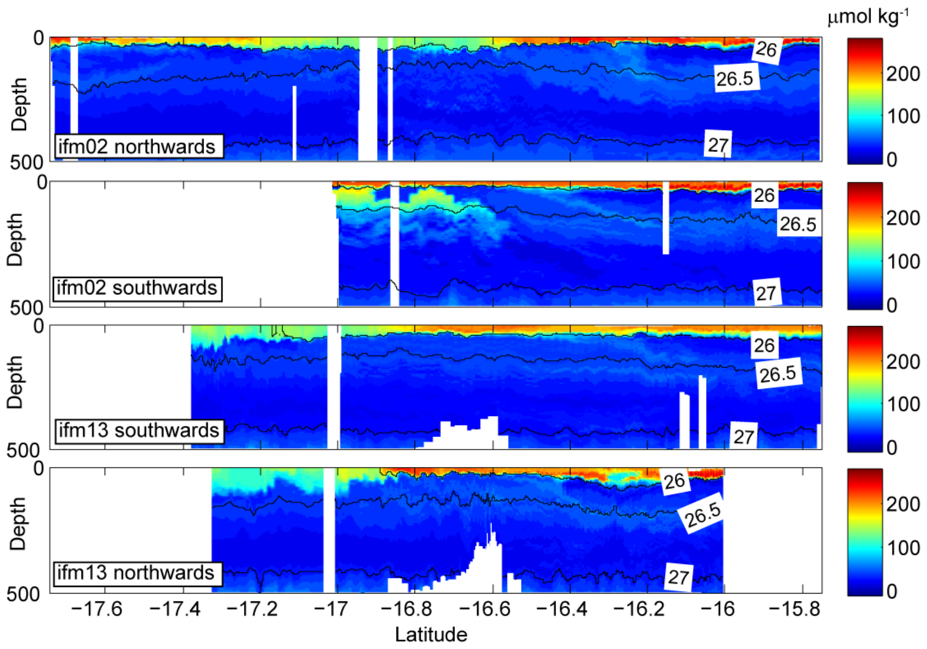

Fig. 5.7: Oxygen (μmol kg^{-1}) distributions across the Angola-Benguela front measured by gliders ifm02 and ifm13. Small-scale oxygen maxima extending from the near-surface to 250 m depth is particularly evident between 16.2°S and 16.6°S. Low near-surface oxygen concentrations indicates upwelling.

5.6 Biochemical measurements

5.6.1 Underway pCO_2, N_2O and CH_4 measurements

(Michael Glockzin, Jan Werner)

During M120 surface water concentrations of the trace gases methane (CH_4), nitrous oxide (N_2O), and carbon dioxide (pCO_2) were measured every 5 seconds. The seawater for the analysis

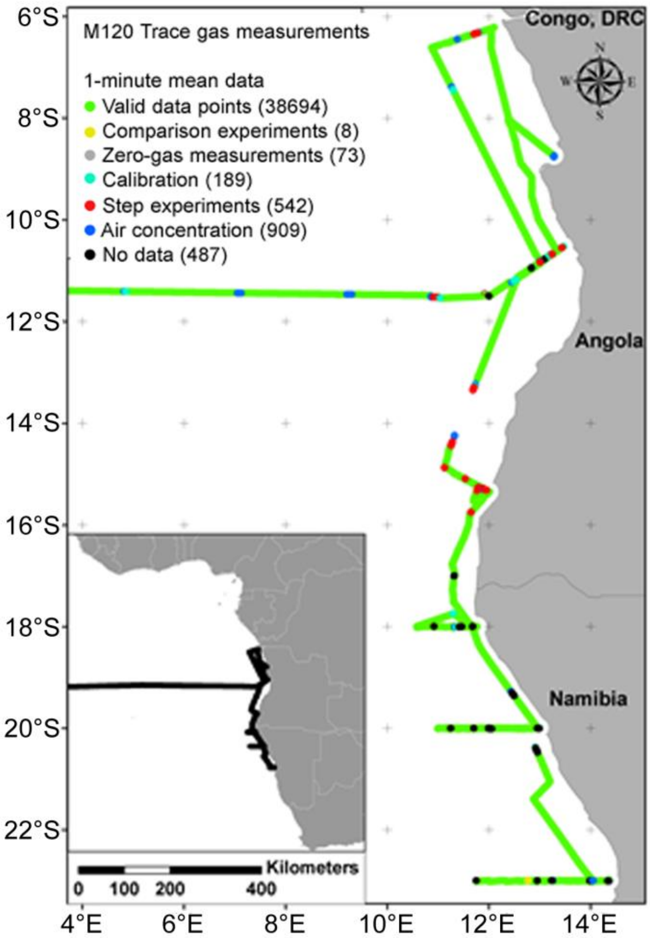

Figure 5.8: Location of surface water and air trace gas concentration measurements and procedures during M120.

was taken from a continuously operating pump installed in the moonpool of METEOR at a water depth of 5 m. The analytical setup consisted of three laser absorption spectroscopy gas analyzers: a CH_4 / CO_2 analyzer (Los Gatos Research / LGR), a N_2O / CO analyzer (LGR), and a $\delta^{13}C$ analyzer (Picarro) for CO_2 concentration measurements. All analyzers were connected to an established custom-built equilibrator setup. The two LGR-analyzers uses off-axis integrated cavity output spectroscopy (OA-ICOS) and the Picarro uses cavity ring down spectroscopy (CRDS). Both methods combine a highly specific infrared band laser with a set of strongly reflective mirrors to obtain an effective laser path length of several kilometers. This allows detecting trace gases and their isotopes in the equilibrated gas phase with high precision and frequency (e.g. Gülzow et al. 2011). The system was frequently checked by standard gas measurements and recalibrated if necessary (Fig. 5.8). To estimate air-sea gas fluxes, trace gas concentration measurements of the ambient air were conducted at different locations during the cruise (Fig. 5.7). For this purpose, tubing was installed on the port side of the vessel.

The surface water concentrations of pCO_2, N_2O and CH_4 together with all related parameters such as temperatures, flow rates of seawater, air volume in equilibrator, were combined with information of the ships' position and UTC time via NMEA string from METEOR's data distributor system. For the calculation of in-situ concentrations of the trace gases, hydrographic and meteorological data were taken from the DSHIP system (inlet at 3.30 m water depth). Analyzer and DSHIP data were combined for the final calculation of one-minute mean values of in-situ gas concentrations to be used for further analysis and mapping. A total of 40,902 one-minute trace gas concentrations (681.6 hours) were measured in the time period of Oct. 18^{th} to Nov. 17, 2015. From these, 487 one-minute averages did not meet the quality control and were removed (Fig. 5.8).

5.6.2 Vertical distribution of N_2O and CH_4

(Jan Werner)

In addition to the underway program ~600 discrete water samples for subsequent measurements of N_2O and CH_4 concentrations were taken at 48 selected stations. The CTD-rosette was stopped for at least 1 Minute during the upcast at specified depths before the water sampler was closed. Samples were filled into 200 mL crimp-top vials, sealed with pretreated butyl rubber stopper, poisoned with 400 µL saturated $HgCl_2$-solution, crimped with aluminum caps, sealed with paraffin and stored at 4°C. Trace gas concentrations will be determined at IOW in Germany.

Water samples were taken at the predominately zonal sections at 6°S, 11°S, 18°S and 23°S and at the meridional 11°E section. The data set will be used to investigate the influence of different waterbodies on trace gas productions. Specifically, it will be tested whether variability of oxygen deficiency, which is controlled by the contribution of various waterbodies, and nutrient inventory including primary production is an important factor for the trace gas flux. For instance, highest N_2O concentrations are expected at hypoxic conditions while highest CH_4 concentrations are expected for anoxic conditions. The latter is known to occur close to the shelf off Namibia (e.g. Monteiro et al. 2006, Naqvi et al. 2010). Furthermore, the dataset will further expand the underway data. Contribution of the underlying water will help to explain surface oversaturation, equilibrium concentrations or undersaturation of N_2O and CH_4.

5.6.3 Nutrient distributions

(Jan Werner, Florian Cordes)

Nutrient concentrations, i.e. ammonium (NH_4^+), nitrate (NO_3^-), nitrite (NO_2^-) and phosphate (PO_4^{3-}), were determined at every 2nd CTD station close to the coast and about every 3rd station in deeper waters (Tab. 7.1). Water samples for nutrient analysis were taken from the Niskin bottles attached to the CTD rosette frame and filled into 0.5 L PE-bottles. The samples were then vacuum-filtrated over GF/F filters and filled in 0.1 L PE-bottles, which were stored at 4°C until nutrient concentrations were analysed.

NH_4^+ was measured manually as indophenol blue with a Shimadzu photometer (UVmini 1240) in an extra lab to avoid contamination e.g. from the analysis of the other nutrients. NO_3^-, NO_2^- and PO_4^{3-} were determined photometrically with a Skalar San++ Autoanalyzer. The chemical procedure of all nutrient measurements followed the procedures detailed in Grasshoff et al. (2009).

The data revealed that in the water column NO_3^- has highest concentrations at 400 m to 500 m depth with maximum values between 40-45 µM in the sampled eastern boundary current system between 6°S and 23°S (not shown). Additionally, surface concentrations are close to 0 µM in the north while elevated concentration as high as 20 µM were observed in the region south of the Angola-Benguela front (Fig. 5.9). Nutrient data will facilitate, inter alia, the interpretation of N_2O concentrations and the related processes such as nitrification and denitrification. Furthermore, the data set will allow distinguishing between different central water masses in the eastern boundary current system.

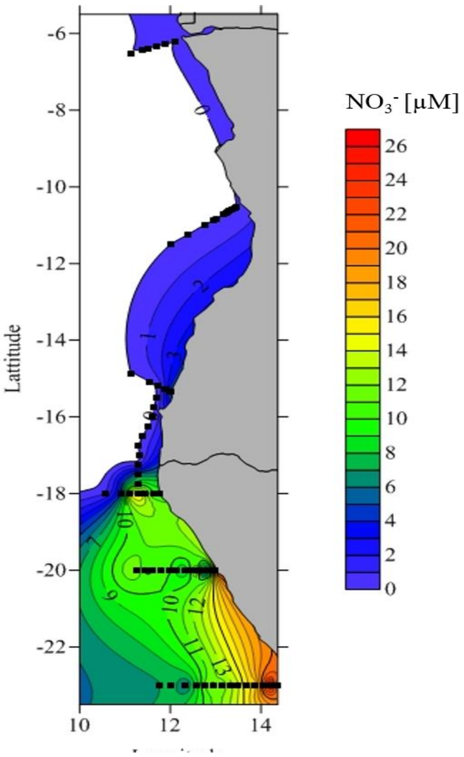

Figure 5.9: Surface concentration of nitrate (NO_3^-). High concentrations are found in the near-coastal regions in the south while values close to 0 µM prevail north of the Angola-Benguela front.

5.6.4 Zooplankton ecology and particle

(Robert Kopte)

An Underwater Vision Profiler 5 (UVP 5) was mounted on the CTD rosette. The instrument consists of one down-facing high density camera in a 6000 dbar pressure-proof case and two red LED lights, which illuminate a 0.93 L-water volume. During the downcast, the UVP takes 3 to 11 pictures of the illuminated field per second. For each picture, the number and size of particles are counted and stored for later data analysis. Furthermore, images of particles with a size > 500 µm are saved as a separate "Vignettes" - small cut-outs of the original picture – which allow for later, computer-assisted identification of these particles and their grouping into different particle, phyto- and zooplankton classes. On the previous cruise M119, one of the two LED lights malfunctioned and was repaired before M120. However, to reduce the risk of damages to the LED, it was decided to operate the UVP only on profiles shallower than 1200m. Therefore, UVP profiles were taken on the CTD profiles 24 to 29, 30, and 33. Unfortunately, the repaired LED light again malfunctioned during CTD profile 34 and could not be repaired. Thus, UVP data is limited to the CTD casts mentioned above.

5.7 Water column backscatter analysis using the multibeam echosounder

(Marek Ostrowski)

High productivity in tropical coastal oceans is generally associated to locations of fronts, upwelling plumes and outflows of major rivers. Temporal and spatial variability of these phenomena controls availability of planktonic prey for pelagic fishes and hence is a critical factor in population dynamic of these species, many of which are of critical commercial importance to coastal economies bordering tropical oceans. Monitoring the change in conditions of the physical environment that may favor or disfavor fish productivity is not easily implementable beyond the largest scales (e.g. SST gradients for satellites) because of the complexity of bio-physical interactions involved; driven largely by a match-mismatch connectivity between fish predation and planktonic pray availability that are controlled at fine- and micro- physical scales. It is therefore worthily to experiment with alternative monitoring techniques that bear a potential to capture this status.

Combining microstructure and fine-scale cross-frontal oceanographic measurements with acoustic imaging has a potential to address this monitoring task. While the oceanographic measurements provide the environmental parameterization of the fine scale, the acoustic observations supply information on locations of fish and plankton aggregations, their composition (if employing sample catches and multi-frequency acoustics) and allow to portrait the kinematics of the water column (through the movements of the passively entrained biota).

The primary aim of the water column backscatter analysis during M120 is to link the patterns of acoustically detected biota concentrations to the oceanographic gradients detected during the survey from the conventional and fine scale oceanographic observations. This has been a very preliminary study, with the biggest challenge being to overcome the limitation on board the METEOR with respect to the acoustic equipment suitable for such a study.

The acoustic observations have been carried out with the Kongsberg Marine EM122 multi-beam echo sounder operating at a frequency of 12 kHz, the only instrument that was accessible to perform this kind of study on board. These multi-beam echo sounders are however optimized for bottom mapping, not for studies of the water column. The adaptation of the output from the echo sounder to water column backscatter observations was associated with a significant methodological challenge and the task could not be fully resolved at the time of this survey due to insufficient technical details known about the particular instrument available on board (a detailed report of the methods and result of the survey can be obtained from M. Ostrowski, mareko@imr.no).

Notwithstanding, the water column data have been collected regularly from October 29 until the end of the survey. All these data were processed and matched to oceanographic patterns. The processed data are stored for further analysis in files using the HDF5 format, a commonly used format to store scientific data.

5.8 Aerosol measurements

(Gerd Logemann)

Aerosol concentration measurements were performed with a handheld MICROTOPS-II sun-photometer in combination with a Garmin GPS unit. GPS fixes are needed to prescribe the available sun-energy above the atmosphere. From the actually measured solar intensity on board METEOR, which is reduced due to absorption and scattering processes in the atmosphere, atmospheric aerosol concentrations and water vapor can be derived. To obtain reliable measurements, a cloud free atmosphere is required. Favorable weather conditions were met during 21 days in which a total of 2600 data points were recorded.

The collected data (Fig. 5.10) offer required ocean reference for satellite remote sensing of aerosol from space and for simulated aerosol properties in global models. The collected data were sent via e-mail to Dr. Smirnov at NASA-GSFC on a daily bases, who also provided immediate feedback on data quality. The data are available at https://aeronet.gsfc.nasa.gov/new_web/ maritime_aerosol_network.html .

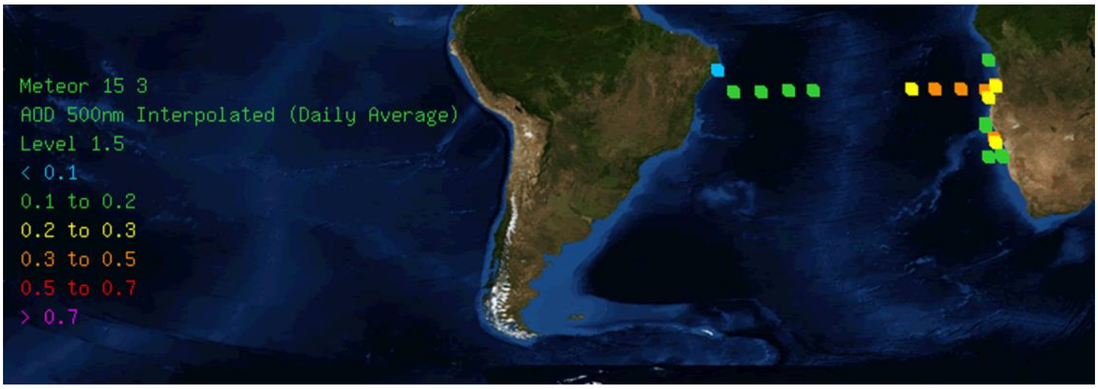

Fig. 5.10 Post-processed daily averages of aerosol concentration measured during M120. The color code represents daily averages of aerosol optical depth (AOD) at the 500nm channel. AOD tells us how much direct sunlight is prevented from reaching the ground by aerosol particles.

6 Weather report and meteorological station

(Carola Heitmann-Bacza, Andreas Raeke)

Weather conditions at the beginning of the cruise and during most of the transatlantic section along 12°S included mostly cloud-free skies, wind from easterly direction of 4 to 5 Bft and a sea state of 1 to 1.5 m with swell from southeast. It was influenced by a subtropical high-pressure area which extended over the Southern Atlantic. The centres (between 1028 hPa and 1032 hPa) moved from the coast of Brazil to east and later south-eastwards to the Cape of Good Hope. A second swell from south to southwest with 1.5 to 2 m arrived at the sailing area between October 21st and 23th. It was caused by a low pressure system which moved south of the high-pressure area to the Cape of Good Hope. After crossing the mid-Atlantic, the daily radio soundings showed a large trade wind temperature inversion in the troposphere that caused a low-level cloud cover while FS METEOR was crossing the eastern part of the Atlantic.

On October 28, shortly before the first mooring activities, a local low pressure system developed temporarily. Air pressure decreased from 1014.1 hPa on October 28, 22:00 UTC to 1009.1 hPa three hours later. Wind refreshed temporarily from light breeze (1-2 Bft.) in the night October 28 to 6 Bft on October 29, 02:00 UTC. However, the low pressure system disintegrated three hours later and thus the first mooring works were accompanied by a light south-westerly breeze, light short showers, 1 m sea and 26°C temperatures.

While surveying in the Angolan territorial waters in the next 10 days, weather conditions were influenced by a trough of a stationary thermal low with a centre across northern Namibia. The low pressure system caused south to south-westerly winds between 3 to 4 Bft. and the sea state was dominated by a southerly swell of 1 to 1.5 m. In addition, a land and sea breeze circulation was pronounced in the coastal regions. One consequence of this were decreasing winds at night, but strengthened southwest to west winds around noon.

While occupying the 20°S section, the south to south-westerly winds increased to 6 Bft between November 7 and 11 and the sea rose up to 3 m by November 12th. Starting with the transit between the 20°S and 23°S section, the weather conditions were influenced by a stationary ridge and a sun strengthening thermal low over Namibia. Strong southeasterly wind of 6 to 7 Bft. and a sea state of about 3 m remained until the evening of November 15. Then, sea state increased to 3.5 to 4 m and swell of 2 to 2.5 m from south to southwest. The water temperature decreased to 13°C when reaching the cold Benguela current and air temperature was usually about 2°C warmer than waters in the mixed layer. After November 15, the high pressure system west of Cape of Good Hope slowly weakened as the associated ridge (1015 hPa) moved westward. Thus, winds decreased. This allowed for the completions of the research program along the 23°S including a successful deployment of the last glider.

7 Lists M120

7.1 Station list

The table uses the following abbreviations: CTD – conductivity, temperature, depth profile measurements, uCTD – underway CTD profile measurements, MSS – microstructure profile measurements, nut – nutrient concentrations determined from water samples.

Station No.		Date	Gear	Time	Latitude	Longitude	Water Depth	Remarks
METEOR (M120-)	GEOMAR	2017		[UTC]	[°]	[°]	[m]	
879-1	uCTD 1	18.10.-20.10.	uCTD	12:08 - 15:41	11°59.91'S	032°26.57'W	4152-4992	**uCTD** transect, 52 profiles
880-1	CTD 1	20.10.	CTD	16:05	11°44.83'S	022°29.23'W	4996	**CTD** station (2000m)
881-1	ARGO 1	20.11.	ARGO	17:33	11°44.83'S	022°29.12'W	5100	**Float** release (WMO #4901428)
882-1	uCTD 2	20.10.-21.10.	uCTD	17:38 - 21:53	11°44.83'S	022°28.67'W	5213 - 4167	**uCTD** transect, 28 profiles
883-1	CTD 2	21.10.	CTD	22:09	11°36.41'S	017°02.17'W	4254	**CTD** station (2000m)
884-1	ARGO 2	21.10.	ARGO	23:45	11°35.97'S	017°01.80'W	4216	**Float** release (WMO #4901429)
885-1	uCTD 3	22.10.-23.10.	uCTD	00:08 -	11°36.10'S	016°59.46'W	3983 – 3946	**uCTD** transect (400m), 34 profiles.
886-1	CTD 3	23.10.	CTD	09:18	11°27.14'S	011°00.26'W	4054	**CTD** station (2000m)
887-1	ARGO 3	23.10.	ARGO	10:52	11°27.25'S	011°00.14'W	4055	**Float** release (WMO #4901682)
888-1	uCTD 4	23.10. - 24.10.	uCTD	11:08 - 18:12	11°27.31'S	010°58.26'W	4061 - 4208	**uCTD** transect (400m), 32 profiles.
889-1	CTD 4	24.10.	CTD	18:20	11°17.77'S	005°00.47'W	4126	**CTD** station (2000m)
890-1	ARGO 4	24.10.	ARGO	20:03	11°17.84'S	005°00.45'W	4105	**Float** release (WMO #4901683)
891-1	uCTD 5	24.10.-26.10.	uCTD	20:14 – 09:10	11°17.79'S	004°59.22'W	4342 - 5601	**uCTD** transect (400m), 38 profiles
892-1	CTD 5	26.10.	CTD	09:23	11°22.47'S	002°00.38' E	5601	**CTD** station (2000m), nut.
893-1	uCTD 6	26.10. – 27.10.	uCTD	11:01 - 21:26	11°22.55'S	002°01.32' E	5604 - 4627	**uCTD** transect (400m), 34 profiles.
894-1	CTD 6	27.10.	CTD	22:07	11°27.74'S	009°00.17'E	4562	**CTD** station (2000m)
895-1	ARGO 5	27.10.	ARGO	23:48	11°27.93'S	009°00.28'E	4543	**Float** release (WMO #3901089)
896-1	uCTD 7	27.10. – 28.10.	uCTD	23:58 - 04:13	11°28.28'S	009°00.79'E	4544-4218	**uCTD** transect (400m), 13 profiles
897-1	ARGO 6	28.10.	ARGO	04:47	11°28.36'S	009°59.96'E	4152	**Float** release (WMO #6902629)
898-1	uCTD 8	28.10.	uCTD	04:58-16:13	11°28.48'S	010°00.78'E	4160 - 3351	**uCTD** transect 8 profs.
899-1	MSS 1	28.10.	MSS	17:50	11°29.24'S	012°00.44'E	2618	**MSS** station (500m)
900-1	CTD 7	28.10.	CTD	18:44	11°29.84'S	012°00.11'E	2602	**CTD** station (bottom), nut.
901-1	MSS 2	28.10.	MSS	23:34	11°14.17'S	012°23.06'E	1851	**MSS** station (500m)
902-1	CTD 8	29.10.	CTD	00:32	11°15.04'S	012°22.51'E	1877	**CTD** station (bottom), nut.
903-1	CTD 9	29.10.	CTD	06:04	10°50.98'S	013°01.06'E	1213	**CTD** station (bottom), nut.
904-1	KPO 1107	29.10.	Mooring	07:43	10°50.00'S	013°00.00'E	1230	**Mooring** recovery
905-1	KPO 1106	29.10.	Mooring	10:28	10°42.57'S	013°11.13'E	500	**Bottom shield** recovery
906-1	CTD 10	29.10.	CTD	13:10	10°41.60'S	013°11.85'E	432	**CTD** station (bottom)
907-1	KPO 1105	29.10.	Mooring	13:54	10°42.10'S	013°11.85'E	400	**Mooring** recovery (unsucessful)
908-1	KPO 1104	29.10.	Mooring	14:53	10°39.72'S	013°15.43'E	183	**Bottom shield** recovery (unsucessful)
909-1	CTD 11	29.10.	CTD	17:36	10°40.57'S	013°14.20'E	295	**CTD** station (bottom), nut.
910-1	MSS 3	29.10.	MSS	18:14	10°40.57'S	013°14.20'E	294	**MSS** station (botttom)
911-1	CTD 12	29.10.	CTD	19:38	10°42.32'S	013°11.39'E	472	**CTD** station (bottom)
912-1	MSS 4	29.10.	MSS	20:08	10°42.32'S	013°11.39'E	471	**MSS** station (bottom)
913-1	CTD 13	29.10.	CTD	21:52	10°43.98'S	013°09.03'E	695	**CTD** station (bottom)
914-1	MSS 5	29.10.	MSS	22:29	10°43.99'S	013°09.03'E	696	**MSS** station (500m)

915-1	CTD 14	30.10.	CTD	00:05	10°46.00’S	013°06.01’E	945	**CTD** station (bottom)
916-1	MSS 6	30.10.	MSS	00:53	10°46.00’S	013°06.00'E	945	**MSS** station (500m)
917-1	CTD 15	30.10.	CTD	02:26	10°47.98’S	013°03.01'E	906	**CTD** station (bottom)
918-1	MSS 7	30.10.	MSS	03:33	10°47.98’S	013°03.00’E	1171	**MSS** station (500m)
919-1	KPO 1105	30.10.	Mooring	07:02	10°41.74’S	013°11.72’E	441	**Mooring** dredging
920-1	KPO 1154	30.10.	Mooring	13:04	10°40.44’S	013°14.44’E	288	**Mooring** PIES deployment
921-1	KPO 1168	30.10.	Mooring	13:31	10°39.71’S	013°15.45’E	200	**Mooring** deployment
922-1	CTD 16	30.10.	CTD	14:11	10°39.21’S	013°16.21’E	162	**CTD** station (bottom), nut.
923-1	MSS 8	30.10.	MSS	14:55	10°39.22’S	013°16.19’E	171	**MSS** station (bottom)
924-1	CTD 17	30.10.	CTD	15:33	10°37.90’S	013°18.22’E	121	**CTD** station (bottom), nut.
925-1	MSS 9	30.10.	MSS	16:02	10°37.92’S	013°18.21’E	120	**MSS** station (bottom)
926-1	MSS 10	30.10.	MSS	17:04	10°39.20’S	013°16.21’E	162	**MSS** station (bottom)
927-1	CTD 18	30.10.	CTD	19:48	10°52.09’S	012°57.03’E	1270	**CTD** station (bottom), nut.
928-1	MSS 11	30.10.	MSS	21:02	10°52.09’S	012°57.03’E	1352	**MSS** station (500m)
929-1	CTD 19	30.10.	CTD	22:49	10°54.02’S	012°54.04’E	1349	**CTD** station (bottom)
930-1	MSS 12	30.10.	MSS	23:54	10°54.05’S	012°53.99’E	1350	**MSS** station (500m)
931-1	CTD 20	31.10.	CTD	01:10	10°56.04’S	012°51.00’E	1376	**CTD** station (bottom)
932-1	MSS 13	31.10.	MSS	02:12	10°56.06’S	012°50.96’E	1373	**MSS** station (500m)
933-1	CTD 21	31.10.	CTD	04:04	10°58.01’S	012°48.00’E	1400	**CTD** station (bottom)
934-1	MSS 14	31.10.	MSS	05:08	10°58.03’S	012°47.99’E	1400	**MSS** station (500m)
935-1	GLI 1	31.10.	Glider	06:51	11°00.04’S	012°45.03’E	1434	**Glider** deployment (IFM03)
936-1	CTD 22	31.10.	CTD	08:46	11°00.02’S	012°45.01’E	1434	**CTD** station (bottom), nut.
937-1	MSS 15	31.10.	MSS	09:38	11°00.03’S	012°44.99’E	1434	**MSS** station (500m)
938-1	CTD 23	31.10.	CTD	15:01	10°31.37’S	013°27.90’E	55	**CTD** station (bottom), nut.
939-1	MSS 16	31.10.	MSS	15:20	10°31.38’S	013°27.89’E	55	**MSS** station (bottom)
940-1	CTD 24	31.10.	CTD	15:59	10°32.89’S	013°25.70’E	75	**CTD** station (bottom), nut.
941-1	MSS 17	31.10.	MSS	16:23	10°32.89’S	013°25.69’E	78	**MSS** station (bottom)
942-1	CTD 25	31.10.	CTD	17:13	10°35.17’S	013°22.19’E	100	**CTD** station (bottom), nut.
943-1	MSS 18	31.10.	MSS	17:38	10°35.18’S	013°22.17’E	101	**MSS** station (bottom)
944-1	CTD 26	02.11.	CTD	09:46	06°12.64’S	012°06.04’E	36	**CTD** station (bottom), nut.
945-1	MSS 19	02.11.	MSS	10:05	06°12.64’S	012°06.04’E	36	**MSS** station (bottom)
946-1	CTD 27	02.11.	CTD	11:22	06°14.91’S	011°59.98’E	61	**CTD** station (bottom)
947-1	MSS 20	02.11.	MSS	11:39	06°14.92’S	011°59.97’E	61	**MSS** station (bottom)
948-1	CTD 28	02.11.	CTD	12:54	06°16.75’S	011°54.01’E	79	**CTD** station (bottom), nut.
949-1	MSS 21	02.11.	MSS	13:22	06°16.75’S	011°54.00’E	80	**MSS** station (bottom)
950-1	CTD 29	02.11.	CTD	14:33	06°18.61’S	011°48.05’E	102	**CTD** station (bottom)
951-1	MSS 22	02.11.	MSS	14:52	06°18.62’S	011°48.01’E	103	**MSS** station (bottom)
952-1	CTD 30	02.11.	CTD	15:58	06°20.38’S	011°42.03’E	116	**CTD** station (bottom), nut.
953-1	MSS 23	02.11.	MSS	16:25	06°20.39’S	011°42.03’E	117	**MSS** station (bottom)
954-1	CTD 31	02.11.	CTD	17:42	06°22.28’S	011°35.97’E	200	**CTD** station (bottom)
955-1	MSS 24	02.11.	MSS	18:02	06°22.28’S	011°35.99’E	201	**MSS** station (bottom)
956-1	CTD 32	02.11.	CTD	19:13	06°24.14’S	011°30.13’E	351	**CTD** station (bottom), nut.
957-1	MSS 25	02.11.	MSS	19:54	06°24.15’S	011°30.12’E	347	**MSS** station (bottom)
958-1	CTD 33	02.11.	CTD	21:29	06°26.60’S	011°22.55’E	541	**CTD** station (bottom), nut.
959-1	MSS 26	02.11.	MSS	22:18	06°26.61’S	011°22.55’E	530	**MSS** station (500m)
960-1	CTD 34	02.11.	CTD	23:48	06°29.09’S	011°15.03’E	845	**CTD** station (bottom)
961-1	MSS 27	03.11.	MSS	00:35	06°29.12’S	011°15.02’E	844	**MSS** station (500m)
962-1	CTD 35	03.11.	CTD	02:09	06°31.51’S	011°07.49’E	1136	**CTD** station (bottom), nut.
963-1	MSS 28	03.11.	MSS	03:23	06°31.52’S	011°07.48’E	1136	**MSS** station (500m)
964-1	CTD 36	03.11.	CTD	04:33	06°33.93’S	011°00.01’E	1453	**CTD** station (bottom)
965-1	CTD 37	03.11.	CTD	06:33	06°36.40’S	010°52.51’E	1676	**CTD** station (bottom)
966-1	uCTD 9	03.11.- 04.11.	uCTD	10:07- 06:11	07°00.78’S	011°04.71’E	1693 - 1136	**uCTD** Transect (400m), 12 profiles
967-1	KPO 1153	04.11.	Mooring	08:50	10°50.00’S	013°00.01’E	1230	**Mooring** deployment
968-1	KPO 1151	04.11.	Mooring	11:57	10°42.13’S	013°11.83’E	444	**Mooring** deployment
969-1	KPO 1168	04.11.	Mooring	13:24	10°39.71’S	013°15.45’E	200	**Mooring** recovery
970-1	KPO 1110	04.11.	Mooring	13:58	10°40.22’S	013°14.64’E	308	**Bottom pressure sensor** recovery
971-1	CTD 38	04.11.	CTD	15:21	10°42.57’S	013°11.13’E	491	**CTD** station (bottom), nut.
972-1	KPO 1152	04.11.	Mooring	16:18	10°42.57’S	013°11.13’E	500	**Bottom shield** deployment
973-1	KPO 1155	04.11.	Mooring	17:32	10°42.68’S	013°11.08’E	500	**PIES** deployment
974-1	MSS 29	04.11.	MSS	17:41	10°42.74’S	013°11.01’E	493	**MSS** station(bottom)
975-1	CTD 39	04.11.	CTD	22:49	11°07.42’S	012°33.83’E	1500	**CTD** station (bottom)
976-1	uCTD 10	05.11.	uCTD	01:01 - 19:10	11°18.83’S	012°29.29’E	1789 – 3114	**uCTD** transect (400m)

977-1	CTD 40	05.11.	CTD	20:14	14°52.46'S	011°07.44'E	3029	**CTD** station (bottom), nut.
978-1	MSS 30	05.11.	MSS	22:38	14°52.46'S	011°07.55'E	3030	**MSS** station (500m)
979-1	CTD 41	06.11.	CTD	00:32	14°58.29'S	011°18.36'E	2792	**CTD** station (bottom)
980-1	MSS 31	06.11.	MSS	02:23	14°58.34'S	011°18.36'E	2803	**MSS** station (500m)
981-1	CTD 42	06.11.	CTD	03:51	15°01.96'S	011°25.22'E	2585	**CTD** station (bottom)
982-1	MSS 32	06.11.	MSS	05:44	15°01.96'S	011°25.21'E	2589	**MSS** station (500m)
983-1	CTD 43	06.11.	CTD	07:19	15°05.58'S	011°32.03'E	1796	**CTD** station (bottom), nut.
984-1	MSS 33	06.11.	MSS	08:50	15°05.60'S	011°32.01'E	1811	**MSS** station (500m)
985-1	CTD 44	06.11.	CTD	10:28	15°09.25'S	011°38.89'E	1778	**CTD** station (bottom)
986-1	MSS 34	06.11.	MSS	11:48	15°09.31'S	011°38.86'E	1782	**MSS** station (500m)
987-1	CTD 45	06.11.	CTD	13:10	15°11.73'S	011°43.45'E	1478	**CTD** station (bottom), nut.
988-1	MSS 35	06.11.	MSS	14:24	15°11.73'S	011°43.45'E	1475	**MSS** station (500m)
989-1	CTD 46	06.11.	CTD	16:06	15°16.63'S	011°52.57'E	600	**CTD** station (bottom), nut.
990-1	MSS 36	06.11.	MSS	17:00	15°16.65'S	011°52.55'E	601	**MSS** station (500m)
991-1	CTD 47	06.11.	CTD	17:58	15°15.38'S	011°50.20'E	842	**CTD** station (bottom)
992-1	MSS 37	06.11.	MSS	18:42	15°15.39'S	011°50.18'E	844	**MSS** station (500m)
993-1	CTD 48	06.11.	CTD	20:15	15°14.23'S	011°47.99'E	1079	**CTD** station (bottom)
994-1	MSS 38	06.11.	MSS	21:07	15°14.24'S	011°47.99'E	1079	**MSS** station (500m)
995-1	CTD 49	06.11.	CTD	23:37	15°30.01'S	011°42.00'E	598	**CTD** station (bottom), nut.
996-1	MSS 39	07.11.	MSS	00:36	15°30.09'S	011°41.99'E	593	**MSS** station (500m)
997-1	CTD 50	07.11.	CTD	04:04	15°17.85'S	011°54.84'E	635	**CTD** station (bottom), nut.
998-1	MSS 40	07.11.	MSS	05:01	15°17.85'S	011°54.81'E	623	**MSS** station (500m)
999-1	CTD 51	07.11.	CTD	06:28	15°19.06'S	011°57.12'E	458	**CTD** station (bottom)
1000-1	MSS 41	07.11.	MSS	06:58	15°19.11'S	011°57.14'E	466	**MSS** station (bottom)
1001-1	CTD 52	07.11.	CTD	08:21	15°20.27'S	011°59.43'E	83	**CTD** station (bottom), nut.
1002-1	MSS 42	07.11.	MSS	08:47	15°20.27'S	011°59.42'E	83	**MSS** station (bottom)
1003-1	CTD 53	07.11.	CTD	09:37	15°20.87'S	012°00.55'E	54	**CTD** station (bottom), nut.
1004-1	MSS 43	07.11.	MSS	09:55	15°20.88'S	012°00.55'E	54	**MSS** station (bottom)
1005-1	GLI 2	07.11.	Glider	13:10	15°44.96'S	011°39.00'E	849	**Glide**r deployment (IFM13)
1006-1	CTD 54	07.11.	CTD	13:59	15°44.97'S	011°39.00'E	853	**CTD** station (bottom), nut.
1007-1	MSS 44	07.11.	MSS	15:03	15°44.98'S	011°38.98'E	862	**MSS** station (500m)
1008-1	uCTD 11	07.11.	uCTD	16:38	15°52.17'S	011°36.97'E	607	**uCTD** Profile (400m)
1009-1	CTD 55	07.11.	CTD	17:23	15°59.97'S	011°36.16'E	420	**CTD** station (bottom), nut.
1010-1	MSS 45	07.11.	MSS	18:06	15°59.99'S	011°36.15'E	597	**MSS** station (500m)
1011-1	uCTD 12	07.11.	uCTD	19:26	16°07.81'S	011°33.26'E	670	**uCTD** Profile (400m)
1012-1	CTD 56	07.11.	CTD	20:19	16°15.26'S	011°30.49'E	361	**CTD** station (bottom), nut.
1013-1	MSS 46	07.11.	MSS	20:52	16°15.30'S	011°30.48'E	330	**MSS** station (bottom)
1014-1	uCTD 13	07.11.	uCTD	22:01	16°22.05'S	011°27.38'E	420	**uCTD** Profile (400m)
1015-1	CTD 57	07.11.	CTD	23:13	16°30.00'S	011°23.43'E	401	**CTD** station (bottom), nut.
1016-1	MSS 47	07.11.	MSS	23:57	16°30.04'S	011°23.42'E	405	**MSS** station (bottom)
1017-1	uCTD 14	08.11.	uCTD	01:17	16°38.29'S	011°20.17'E	315	**uCTD** Profile (300m)
1018-1	CTD 58	08.11.	CTD	02:06	16°45.00'S	011°17.30'E	453	**CTD** station (bottom), nut.
1019-1	MSS 48	08.11.	MSS	02:44	16°45.20'S	011°17.32'E	443	**MSS** station (bottom)
1020-1	uCTD 15	08.11.	uCTD	04:03	16°52.66'S	011°18.35'E	570	**uCTD** Profile (300m)
1021-1	CTD 59	08.11.	CTD	04:50	17°00.11'S	011°19.12'E	590	**CTD** station (bottom), nut.
1022-1	MSS 49	08.11.	MSS	05:19	17°00.12'S	011°18.95'E	480	**MSS** station (bottom)
1023-1	uCTD 16	08.11.	uCTD	06:47	17°09.39'S	011°17.92'E	441	**uCTD** Profile (400m)
1024-1	CTD 60	08.11.	CTD	07:29	17°14.93'S	011°17.27'E	652	**CTD** station (bottom), nut.
1025-1	MSS 50	08.11.	MSS	08:07	17°14.94'S	011°17.27'E	498	**MSS** station (bottom)
1026-1	uCTD 17	08.11.	uCTD	09:44	17°24.14'S	011°18.01'E	173	**uCTD** Profile (100m)
1027-1	CTD 61	08.11.	CTD	10:25	17°29.94'S	011°18.35'E	700	**CTD** station (bottom), nut.
1028-1	MSS 51	08.11.	MSS	10:56	17°29.95'S	011°18.35'E	217	**MSS** station (bottom)
1029-1	uCTD 18	08.11.	uCTD	12:33	17°40.56'S	011°25.40'E	226	**uCTD** transect, 3 profiles.
1030-1	LTKC	08.11.	Mooring	14:47	18°00.00'S	011°39.00'E	125	**Bottom shield** recovery
1031-1	CTD 62	08.11.	CTD	18:39	17°59.96'S	011°45.99'E	50	**CTD** station (bottom), nut.
1032-1	MSS 52	08.11.	MSS	18:55	18°00.00'S	011°46.00'E	51	**MSS** station (bottom)
1033-1	CTD 63	08.11.	CTD	19:52	18°00.00'S	011°42.88'E	89	**CTD** station (bottom), nut.
1034-1	MSS 53	08.11.	MSS	20:15	18°00.01'S	011°42.88'E	88	**MSS** station (bottom)
1035-1	CTD 64	08.11.	CTD	21:33	17°59.93'S	011°37.98'E	126	**CTD** station (bottom), nut.
1036-1	MSS 54	08.11.	MSS	21:54	17°59.96'S	011°37.98'E	126	**MSS** station (bottom)
1037-1	CTD 65	08.11.	CTD	23:03	17°59.98'S	011°34.97'E	182	**CTD** station (bottom)
1038-1	MSS 55	08.11.	MSS	23:24	18°00.01'S	011°34.97'E	182	**MSS** station (bottom)
1039-1	CTD 66	09.11.	CTD	00:35	17°59.97'S	011°30.99'E	231	**CTD** station (bottom)
1040-1	MSS 56	09.11.	MSS	00:57	17°59.99'S	011°30.99'E	230	**MSS** station (bottom)
1041-1	CTD 67	09.11.	CTD	02:10	17°59.99'S	011°26.97'E	274	**CTD** station (bottom), nut.

1042-1	MSS 57	09.11.	MSS	02:45	18°00.02'S	011°26.98'E	275	**MSS** station (bottom)
1043-1	CTD 68	09.11.	CTD	03:58	17°59.95'S	011°21.95'E	550	**CTD** station (bottom), nut.
1044-1	MSS 58	09.11.	MSS	04:43	17°59.95'S	011°21.95'E	556	**MSS** station (500m)
1045-1	HRKC	09.11.	Mooring	07:18	17°59.60'S	011°38.84'E	125	**Mooring** deployment
1046-1	GLI 3	09.11.	Glider	10:10	17°44.84'S	011°17.73'E	772	**Glider** deployment (failed)
1047-1	CTD 69	09.11.	CTD	10:33	17°44.82'S	011°17.68'E	778	**CTD** station (bottom), nut.
1048-1	GLI 4	09.11.	Glider	11:32	17°44.83'S	011°17.63'E	786	**Glider** deployment (IFM02)
1049-1	MSS 59	09.11.	MSS	12:30	17°44.90'S	011°17.26'E	835	**MSS** station (500m)
1050-1	CTD 70	09.11.	CTD	17:00	17°59.98'S	010°34.97'E	3492	**CTD** station (bottom), nut.
1051-1	MSS 60	09.11.	MSS	19:41	18°00.00'S	010°34.97'E	3492	**MSS** station (500m)
1052-1	CTD 71	09.11.	CTD	22:32	17°59.91'S	010°55.01'E	2790	**CTD** station (bottom), nut.
1053-1	MSS 61	10.11.	MSS	00:44	17°59.92'S	010°55.01'E	2805	**MSS** station (500m)
1054-1	CTD 72	10.11.	CTD	02:48	17°59.98'S	011°06.98'E	1971	**CTD** station (bottom), nut.
1055-1	MSS 62	10.11.	MSS	04:32	18°00.01'S	011°06.99'E	2077	**MSS** station (500m)
1056-1	CTD 73	10.11.	CTD	06:18	17°59.96'S	011°16.96'E	1014	**CTD** station (bottom), nut.
1057-1	MSS 63	10.11.	MSS	07:52	18°00.54'S	011°17.28'E	995	**MSS** station (500m)
1058-1	CTD 74	10.11.	CTD	09:06	17°59.85'S	011°19.51'E	761	**CTD** station (bottom)
1059-1	MSS 64	10.11.	MSS	09:48	17°59.86'S	011°19.51'E	758	**MSS** station (500m)
1060-1	HRKC	10.11.	Mooring	12:41	17°59.60'S	011°38.84'E	125	**Mooring** recovery
1061-1	LTKC	10.11.	Mooring	13:42	18°00.00'S	011°39.00'E	125	**Bottom shield** deployment
1062-1	CTD 75	11.11.	CTD	04:00	19°59.98'S	012°59.55'E	32	**CTD** station (bottom), nut.
1063-1	MSS 65	11.11.	MSS	04:15	20°00.01'S	012°59.54'E	32	**MSS** station (bottom)
1064-1	CTD 76	11.11.	CTD	04:56	19°59.97'S	012°57.08'E	53	**CTD** station (bottom), nut.
1065-1	MSS 66	11.11.	MSS	05:15	19°59.99'S	012°57.07'E	55	**MSS** station (bottom),
1066-1	CTD 77	11.11.	CTD	06:11	20°00.01'S	012°50.95'E	98	**CTD** station (bottom), nut.
1067-1	MSS 67	11.11.	MSS	06:31	20°00.03'S	012°50.94'E	99	**MSS** station (bottom)
1068-1	CTD 78	11.11.	CTD	07:40	19°59.98'S	012°44.96'E	119	**CTD** station (bottom), nut.
1069-1	MSS 68	11.11.	MSS	08:23	19°59.99'S	012°44.96'E	117	**MSS** station (bottom)
1070-1	LTTB	11.11.	Mooring	09:15	19°59.97'S	012°44.98'E	125	**Bottom shield** recovery
1071-1	HRTB	11.11.	Mooring	10:09	19°59.91'S	012°44.96'E	125	**Mooring** deployment
1072-1	CTD 79	11.11.	CTD	10:57	19°59.94'S	012°40.96'E	125	**CTD** station (bottom), nut.
1073-1	MSS 69	11.11.	MSS	11:30	19°59.99'S	012°40.95'E	126	**MSS** station (bottom)
1074-1	CTD 80	11.11.	CTD	12:39	20°00.00'S	012°35.53'E	135	**CTD** station (bottom), nut.
1075-1	MSS 70	11.11.	MSS	13:08	20°00.05'S	012°35.52'E	135	**MSS** station (bottom)
1076-1	CTD 81	11.11.	CTD	14:19	19°59.99'S	012°30.01'E	151	**CTD** station (bottom), nut.
1077-1	MSS 71	11.11.	MSS	14:45	20°00.02'S	012°30.01'E	151	**MSS** station (bottom)
1078-1	CTD 82	11.11.	CTD	15:52	19°59.97'S	012°25.02'E	196	**CTD** station (bottom), nut.
1079-1	MSS 72	11.11.	MSS	16:15	19°59.97'S	012°25.02'E	196	**MSS** station (bottom)
1080-1	CTD 83	11.11.	CTD	17:23	19°59.98'S	012°20.02'E	213	**CTD** station (bottom), nut.
1081-1	MSS 73	11.11.	MSS	17:46	19°59.99'S	012°20.02'E	213	**MSS** station (bottom)
1082-1	CTD 84	11.11.	CTD	18:48	19°59.99'S	012°14.97'E	247	**CTD** station (bottom), nut.
1083-1	MSS 74	11.11.	MSS	19:08	20°00.00'S	012°14.97'E	248	**MSS** station (bottom)
1084-1	CTD 85	11.11.	CTD	20:27	19°59.97'S	012°08.89'E	283	**CTD** station (bottom), nut.
1085-1	MSS 75	11.11.	MSS	20:55	19°59.98'S	012°08.89'E	283	**MSS** station (bottom)
1086-1	CTD 86	11.11.	CTD	22:16	19°59.84'S	012°03.84'E	312	**CTD** station (bottom), nut.
1087-1	MSS 76	11.11.	MSS	22:46	19°59.86'S	012°03.84'E	312	**MSS** station (bottom)
1088-1	CTD 87	12.11.	CTD	00:09	19°59.98'S	011°58.36'E	348	**CTD** station (bottom), nut.
1089-1	MSS 77	12.11.	MSS	00:41	20°00.01'S	011°58.35'E	347	**MSS** station (bottom)
1090-1	CTD 88	12.11.	CTD	02:04	19°59.99'S	011°52.58'E	388	**CTD** station (bottom)
1091-1	MSS 78	12.11.	MSS	02:31	19°59.99'S	011°52.56'E	386	**MSS** station (bottom)
1092-1	CTD 89	12.11.	CTD	03:42	20°00.00'S	011°46.74'E	453	**CTD** station (bottom)
1093-1	MSS 79	12.11.	MSS	04:14	20°00.02'S	011°46.80'E	453	**MSS** station (bottom)
1094-1	CTD 90	12.11.	CTD	05:28	19°59.99'S	011°41.94'E	545	**CTD** station (bottom)
1095-1	MSS 80	12.11.	MSS	05:58	20°00.00'S	011°41.94'E	544	**MSS** station (500m)
1096-1	CTD 91	12.11.	CTD	07:11	19°59.96'S	011°36.94'E	639	**CTD** station (bottom), nut.
1097-1	MSS 81	12.11.	MSS	08:00	19°59.99'S	011°36.95'E	646	**MSS** station (500m)
1098-1	CTD 92	12.11.	CTD	09:53	20°00.00'S	011°26.26'E	845	**CTD** station (bottom), nut.
1099-1	MSS 82	12.11.	MSS	10:40	20°00.00'S	011°26.25'E	842	**MSS** station (500m)
1100-1	CTD 93	12.11.	CTD	12:49	20°00.00'S	011°14.99'E	1050	**CTD** station (bottom), nut.
1101-1	MSS 83	12.11.	MSS	13:52	20°00.04'S	011°14.98'E	1051	**MSS** station (500m)
1102-1	CTD 94	12.11.	CTD	15:51	19°59.97'S	010°59.99'E	1272	**CTD** station (bottom)
1103-1	MSS 84	12.11.	MSS	16:48	19°59.99'S	010°59.98'E	1274	**MSS** station (500m)
1104-1	MSS 85	13.11.	MSS	03:33	20°00.11'S	012°44.92'E	120	**MSS** station (bottom)
1105-1	HRTB	13.11.	Mooring	06:52	19°59.91'S	012°44.96'E	125	**Mooring** recovery (125m)
1106-1	LRTB	13.11.	Mooring	08:08	19°59.97'S	012°44.98'E	125	Bottom shield deployment

1107-1	CTD 95	14.11.	CTD	09:52	22°59.65'S	014°02.19'E	134	**CTD** station (bottom)
1108-1	HRMB	14.11.	Mooring	10:16	22°59.98'S	014°02.27'E	132	**Mooring** deployment
1109-1	CTD 96	14.11.	CTD	12:42	22°59.99'S	014°22.00'E	40	**CTD** station (bottom), nut.
1110-1	MSS 86	14.11.	MSS	13:00	23°00.03'S	014°21.99'E	41	**MSS** station (bottom)
1111-1	CTD 97	14.11.	CTD	13:54	22°59.98'S	014°19.02'E	70	**CTD** station (bottom), nut.
1112-1	MSS 87	14.11.	MSS	14:12	22°59.99'S	014°19.02'E	72	**MSS** station (bottom)
1113-1	CTD 98	14.11.	CTD	15:22	22°59.96'S	014°13.00'E	109	**CTD** station (bottom), nut.
1114-1	MSS 88	14.11.	MSS	15:40	22°59.98'S	014°13.00'E	109	**MSS** station (bottom)
1115-1	CTD 99	14.11.	CTD	16:48	22°59.95'S	014°07.95'E	136	**CTD** station (bottom)
1116-1	MSS 89	14.11.	MSS	17:04	22°59.94'S	014°07.91'E	135	**MSS** station (bottom)
1117-1	CTD 100	14.11.	CTD	18:07	22°59.98'S	014°03.49'E	132	**CTD** station (bottom), nut.
1118-1	MSS 90	14.11.	MSS	18:27	22°59.99'S	014°03.49'E	130	**MSS** station (bottom)
1119-1	CTD 101	14.11.	CTD	19:48	22°59.94'S	013°57.49'E	140	**CTD** station (bottom)
1120-1	MSS 91	14.11.	MSS	20:03	22°59.95'S	013°57.49'E	140	**MSS** station (bottom)
1121-1	CTD 102	14.11.	CTD	21:18	22°59.95'S	013°51.97'E	144	**CTD** station (bottom), nut.
1122-1	MSS 92	14.11.	MSS	21:37	22°59.96'S	013°51.97'E	145	**MSS** station (bottom)
1123-1	CTD 103	14.11.	CTD	22:52	22°59.92'S	013°46.46'E	146	**CTD** station (bottom)
1124-1	MSS 93	14.11.	MSS	23:12	22°59.93'S	013°46.46'E	145	**MSS** station (bottom)
1125-1	CTD 104	15.11.	CTD	10:05	22°59.94'S	011°44.92'E	3000	**CTD** station (bottom), nut.
1126-1	MSS 94	15.11.	MSS	12:18	22°59.96'S	011°44.92'E	2999	**MSS** station (500m)
1127-1	ARGO 7	15.11.	ARGO	13:02	23°00.35'S	011°44.98'E	2996	**Float** release (WMO # 6902630)
1128-1	CTD 105	15.11.	CTD	14:39	22°59.99'S	011°59.96'E	2715	**CTD** station (bottom), nut.
1129-1	MSS 95	15.11.	MSS	16:47	23°00.01'S	011°59.96'E	2712	**MSS** station (500m)
1130-1	ARGO 8	15.11.	ARGO	17:23	23°00.74'S	012°00.05'E	2907	**Float** release (WMO #6902631)
1131-1	CTD 106	15.11.	CTD	19:29	22°59.96'S	012°20.02'E	2070	**CTD** station (bottom), nut.
1132-1	MSS 96	15.11.	MSS	21:07	22°59.98'S	012°20.02'E	2072	**MSS** station (500m)
1133-1	CTD 107	15.11.	CTD	23:27	23°00.00'S	012°35.02'E	1433	**CTD** station, nut.
1134-1	MSS 97	16.11.	MSS	00:47	23°00.01'S	012°35.02'E	1431	**MSS** station (500m)
1135-1	LTMB	16.11.	Mooring	08:42	23°01.00'S	014°02.20'E	132	**Sediment trap** recovery
1136-1	LTMB	16.11.	Mooring	10:04	22°59.81'S	014°02.36'E	132	**Mooring** recovery
1137-1	CTD 108	16.11.	CTD	13:01	22°59.98'S	013°41.02'E	150	**CTD** station (bottom), nut.
1138-1	CTD 109	16.11.	CTD	14:30	22°59.96'S	013°29.88'E	289	**CTD** station (bottom), nut.
1139-1	GLI 5	16.11.	Glider	15:59	22°59.94'S	013°19.00'E	359	**Glider** deployment (IFM09)
1140-1	CTD 110	16.11.	CTD	16:46	23°00.00'S	013°18.99'E	360	**CTD** station (bottom), nut.
1141-1	MSS 98	16.11.	MSS	17:19	23°00.01'S	013°18.99'E	348	**MSS** station (bottom)
1142-1	CTD 111	16.11.	CTD	18:51	22°59.99'S	013°07.98'E	319	**CTD** station (bottom), nut.
1143-1	MSS 99	16.11.	MSS	19:25	23°00.05'S	013°07.98'E	318	**MSS** station (bottom)
1144-1	CTD 112	16.11.	CTD	21:20	23°00.00'S	012°56.82'E	728	**CTD** station (bottom), nut.
1145-1	MSS 100	16.11.	MSS	22:06	23°00.00'S	012°56.82'E	601	**MSS** station (500m)
1146-1	CTD 113	16.11.	CTD	23:51	23°00.01'S	012°46.01'E	985	**CTD** station (bottom), nut.
1147-1	MSS 101	17.11.	MSS	00:59	23°00.01'S	012°46.01'E	989	**MSS** station (500m)
1148-1	MSS 102	17.11.	MSS	05:30	23°00.05'S	013°30.03'E	237	**MSS** station (bottom)
1149-1	CTD 114	17.11.	CTD	06:42	22°59.97'S	013°35.49'E	148	**CTD** station (bottom)
1150-1	MSS 103	17.11.	MSS	07:00	23°00.01'S	013°35.49'E	149	**MSS** station (bottom)
1151-1	MSS 104	17.11.	MSS	08:10	22°59.97'S	013°41.02'E	151	**MSS** station (bottom)
1152-1	LTMB	17.11.	Mooring	10:35	22°59.81'S	014°02.36'E	132	**Mooring** deployment
1153-1	HRMB	17.11.	Mooring	11:02	22°59.98'S	014°02.27'E	132	**Mooring** recovery
1154-1	LTMB	17.11.	Mooring	12:00	23°01.00'S	014°02.20'E	135	**Sediment trap** deployment

7.2 List of moorings

7.2.1 Moorings deployments and recoveries in Angolan waters.

Mooring recovery: Angola bottom shield						**Notes:**	**KPO 1104**
Vessel:	Meteor	M98					
Deployed:	22-Jul	2013					
Vessel:							
Recovered:							
Latitude:		10	39.718	S			
Longitude:		13	15.428	E			
Water depth:	200m		Mag Var:		-5.4		

ID	Depth	Instr. Type	s/n	Start-up	Remarks
		Argos	5461		
KPO_1106_01	200	ADCP 150kHz	14912	X	Not recovered
	200	Release	1641	Code:	no response on 29-Oct-2015
	200	Shield	JOB129-001	Code:	

Mooring deployments: Angola T, S, P, O_2 logger mooring					**Notes:**	**KPO 1105**
Vessel:	Meteor	M98				
Deployed:	23-Jul	2013	12:52			
Vessel:						
Recovered:						
Latitude:		10	42.104	S		
Longitude:		13	11.852	E		
Water depth:	450m	Mag Var:		-5.4		

ID	Depth	Instr. Type	s/n	Start-up	Remarks
		Argos	5639		Not recovered
KPO_1105_01	50	MC-P	10631	X	Not recovered
KPO_1105_02	50	O_2-Logger	1139	X	Not recovered
KPO_1105_03	153	MC-P	10611	X	Not recovered
KPO_1105_04	153	O_2-Logger	145	X	Not recovered
KPO_1105_05	247	MC	1284	X	Not recovered
KPO_1105_06	247	O_2-Logger	1067	X	Not recovered
KPO_1105_07	352	MC-P	10630	X	Not recovered
KPO_1105_08	352	O_2-Logger	531	X	Not recovered
	375	Release AR661	121	Code:	no response on 29-Oct-2015

Mooring recovery: Angola bottom shield					**Notes:**	**KPO 1106**
Vessel:	Meteor	M98				
Deployed:	23-Jul	2013				
Vessel:	Meteor	M120				
Recovered:	29-Oct	2015				
Latitude:		10	42.774	S		
Longitude:		13	11.131	E		
Water depth:	498m	Mag Var:		-4.9		

ID	Depth	Instr. Type	s/n	Start-up	Remarks
		Argos	5507		
KPO_1106_01	498	ADCP LR 75kHz	19397	X	complete and clean record
	498	SBE 26plus	1356	X	complete and clean record
	498	Release	1591	Code:	
	498	Shield	JOB183-001	Code:	

Mooring recovery: ADCP mooring					**Notes:**	**KPO 1107**
Vessel:	Meteor	M98				
Deployed:	23-Jul	2013				
Vessel:	Meteor	M120				
Recovered:	29-Oct	2015				
Latitude:		10	50.000	S		
Longitude:		13	00.000	E		
Water depth:	1230m	Mag Var:		-5.0		

ID	Depth	Instr. Type	s/n	Start-up	Remarks
		SMM2000	9243		
KPO_1107_01	505	ADCP LR up	19398	X	complete and clean record

	1125	Release AR661	189	Code:	

Mooring recovery: Angola bottom pressure sensor				**Notes:**	**KPO 1110**
Vessel:	Meteor	M98			
Deployed:	22-Jul	2013			
Vessel:	Meteor	M120			
Recovered:	29-Oct	2015			
Latitude:		10	40.443	S	
Longitude:		13	14.433	E	
Water depth:	303m				
ID	**Depth**	**Instr. Type**	**s/n**	**Start-up**	**Remarks**
		Animate 8B	9243		
KPO_1110_01	303	SBE 26plus	1355	**X**	complete and clean record
	303	Releaser 865A	652	Code:	

Mooring deployment and recovery: double ADCP mooring					**Notes:**	**KPO 1168**
Vessel:	Meteor	M120				
Deployed:	30-Oct	2015	13:45			
Vessel:	Meteor	M120				
Recovered:	04-Nov	2015	13:40			
Latitude:		10	39.710	S		
Longitude:		13	15.450	E		
Water depth:	200m		Mag Var:	-4.7		
ID	**Depth**	**Instr. Type**	**s/n**	**Start-up**	**Remarks**	
KPO_1168_01	171	ADCP WH 300up	1522	**X**	complete and clean record	
KPO_1168_02	171	ADCP WH 1200dwn	7279	**X**	complete and clean record	
	195	Releaser RT661	041	Code:		

Mooring deployments: Angola T, S, P, O_2 logger mooring					**Notes:**	**KPO 1151**
Vessel:	Meteor	M120				
Deployed:	04-Nov	2015	12:52			
Vessel:						
Recovered:						
Latitude:		10	42.129	S		
Longitude:		13	11.830	E		
Water depth:	444m		Mag Var:	-4.7		
ID	**Depth**	**Instr. Type**	**s/n**	**Start-up**	**Remarks**	
	24	Argos	2265			
KPO_1151_01	48	MC-P	6861	**X**		
KPO_1151_02	48	O_2-Logger	1462	**X**		
KPO_1151_03	151	MC-P	6862	**X**		
KPO_1151_04	151	O_2-Logger	1468	**X**		
KPO_1151_05	245	MC	2048	**X**		
KPO_1151_06	245	O_2-Logger	1143	**X**		
KPO_1151_07	350	MC-P	6856	**X**		
KPO_1151_08	350	O_2-Logger	1155	**X**		
	436	Release AR661	635	Code:		

Mooring deployments: Angola bottom shield				**Notes:**	**KPO 1152**
Vessel:	Meteor	M120			
Deployed:	04-Nov.	2015	17:20		

Vessel:						
Recovered:						
Latitude:		10	42.571	S		
Longitude:		13	11.130	E		
Water depth:	491m		Mag Var:	-4.9		
ID	**Depth**	**Instr. Type**	**s/n**	**Start-up**	**Remarks**	
		Argos	5507			
KPO_1152_01	491	ADCP LR 75kHz	19397	**X**		
	491	SBE 26plus	1356	**X**		
	491	Release	1591	Code:		
	491	Shield	JO8183-001	Code:		

Mooring deployments: Angola ADCP mooring					**Notes:**	**KPO 1153**
Vessel:	Meteor	M120				
Deployed:	04-Nov	2015	09:57			
Vessel:						
Recovered:						
Latitude:		10	50.001	S		
Longitude:		13	00.007	E		
Water depth:	1228m		Mag Var:	-5.0		
ID	**Depth**	**Instr. Type**	**s/n**	**Start-up**	**Remarks**	
		SMM2000	9243			
KPO_1153_01	498	ADCP LR up	19398	**X**		
	1220	Release AR661	642	Code:		

Mooring deployment: Pressure inverted echo sounder					**Notes:**	**KPO 1154**
Vessel:	Meteor	M120				
Deployed:	30-Oct	2015	13:10			
Vessel:						
Recovered:						
Latitude:		10	40.443	S		
Longitude:		13	14.439	E		
Water depth:	288m					
ID	**Depth**	**Instr. Type**	**s/n**	**Start-up**	**Remarks**	
KPO_1154_01	288	PIES	113	**X**		

Mooring deployment: Pressure inverted echo sounder					**Notes:**	**KPO 1155**
Vessel:	Meteor	M120				
Deployed:	04-Nov	2015	17:40			
Vessel:						
Recovered:						
Latitude:		10	42.682	S		
Longitude:		13	11.085	E		
Water depth:	491m					
ID	**Depth**	**Instr. Type**	**s/n**	**Start-up**	**Remarks**	
KPO_1155_01	491	PIES	165	**X**		

7.2.2 Long-term mooring positions and deployment times of the Namibian coast.

Name	Depth	Latitude	Longitude	deployed	recovered	Comment
LTKC_04	124	17°59.989'S	11°40.793'E	*26.01.2015*	08.11.2015	dredged, 2 trials
LTKC_05	125	17°59.985'S	11°38.997'E	10.11.2015	*May 2016*	ADCP-shield
	125	17°59.970'S	11°39.067'E	10.11.2015	*May 2016*	End of ground rope
LTTB_04	125	20°00.028'S	12°45.100'E	*26.01.2015*	11.11.2015	release ok
LTTB_05	118	19°59.957'S	12°44.982'E	13.11.2015	*May 2016*	ADCP-shield
	118	19°59.965'S	12°45.085'E	13.11.2015	*May 2016*	End of ground rope
LTMB_11	130	23°00.046`S	14°02.817`E	*26.01.2015*	16.11.2015	Second release!
LTMB_12	130	22°59.897`S	14°02.965`E	17.11.2015	*May 2016*	ADCP-shield
	130	22°59.896`S	14°02.907`E	17.11.2015	*May 2016*	End of ground rope

7.2.3 High resolution mooring positions and deployment times.

Name	Depth	Latitude	Longitude	deployed	recovered	Comment
HR_120_1	124	17°59.610'S	11°38.843'E	09.11.2015	10.11.2015	mooring
	124	17°59.669'S	11°38.365'E	09.11.2015	10.11.2015	End of ground rope
HR_120_2	125	19°59.892'S	12°44.965'E	11.11.2015	13.11.2015	mooring
	125	19°59.973'S	12°44.979'E	11.11.2015	13.11.2015	End of ground rope
HR_120_3	128	22°59.975'S	14°02.273'E	14.11.2015	17.11.2015	mooring
	128	23°00.007'S	14°02.276'E	14.11.2015	17.11.2015	End of ground rope

7.3 MSS Profiles and shear sensors

List of shear sensors mounted on the MSS profiler during the cruise.

	Profiles	She1 – sensor			She2 – sensor		
		Type	No	Sensitivity	Type	No	Sensitivity
Sensor test	001 – 005	A	69	0.0004040	A	32	0.0003900
Sensor test	006 – 008	A	69	0.0004040	C	SG001	0.0000505
Lobito transect 11°S	009 – 071	C	SG002	0.0000538	C	SG001	0.0000505
Kongo transect 06°S	072 – 121	A	32	0.0003900	C	SG001	0.0000505
Sensor test	122 – 123	B	8002	0.0008180	C	SG001	0.0000505
Namibe transect 15°S	124 – 161	B	8002	0.0008180	C	SG001	0.0000505
ABFZ transect	162 – 179	C	SG002	0.0000538	C	SG001	0.0000505
Kunene transect 18°S	180 – 220	C	SG002	0.0000538	C	SG001	0.0000505
Terrace Bay transect 20°S	221 – 325	C	SG002	0.0000538	C	SG001	0.0000505
Walvis Bay transect 23°S	326 – 400	C	SG002	0.0000538	A	32	0.0003900

8 Data and Sample Storage and Availability

In Kiel, a joint data management team is set up to store the data from various projects and cruises in a web-based multi-user-system. Data gathered during M120 are stored at the Kiel data portal, and remain proprietary for the PIs of the cruise and for members of EU-PREFACE and the BMBF-SACUS project for a period of 3 years after the cruise. Each station is logged as an event file https://portal.geomar.de/metadata/leg/show/333353. All data will be submitted to the world data center PANGAEA within 3 years after the cruise, i.e. by December 2018. There, the data will be freely available. Preliminary CTD data were submitted to CORIOLIS during the cruise for real time oceanographic analysis and Argo calibration. Contact persons for the different datasets are listed in Table 8.1.

Tab. 8.1: Overview of contact persons for the different data sets.

Data	Contact Person	Current Affiliation	Email
CTD/O_2	Dr. Marcus Dengler	GEOMAR	mdengler@geomar.de
VMADCP	Dr. Marcus Dengler	GEOMAR	mdengler@geomar.de
LADCP	Dr. Marcus Dengler	GEOMAR	mdengler@geomar.de
Mooring data Angola	Dr. Marcus Dengler	GEOMAR	mdengler@geomar.de
Mooring data Namibia	Dr. Volker Mohrholz	IOW	volker.mohrholz@io-warnemuende.de
Microstructure data	Dr. Volker Mohrholz	IOW	volker.mohrholz@io-warnemuende.de
Underway CO_2, CH_4, N_2O, CO, $\delta^{13}C$	Prof. Dr. Gregor Rehder	IOW	gregor.rehder@io-warnemuende.de
Nutrients	Prof. Dr. Gregor Rehder	IOW	gregor.rehder@io-warnemuende.de
Thermosalinograph	Dr. Marcus Dengler	GEOMAR	mdengler@geomar.de
Underway CTD profiles	Dr. Marcus Dengler	GEOMAR	mdengler@geomar.de
Multibeam echosounder	Prof. Dr. Colin Devey	GEOMAR	cdevey@geomar.de
Multibeam echosounder watercolumn data	Dr. Marek Ostrowski	IMR	mareko@imr.no

9 Acknowledgements

We are grateful to Capitan Hammacher und his crew for the excellent collaboration and the pleasant working atmosphere during the cruise. The crew of METEOR greatly contributed to the success of the cruise. The ship time of METEOR was provided by the German Science Foundation (DFG) within the core program METEOR/MERIAN. Financial support was provided by the German Federal Ministry of Education and Research (BMBF) as part of the cooperative project SACUS „Southwest African Coastal Upwelling System and Benguela Niños“(03V01295) and by EU funded collaborative project PREFACE „Enhancing prediction of tropical Atlantic climate and its impacts“ (Grant No 603521).

10 References

Grasshoff, K., Kremling, K., Ehrhardt, M., eds. *Methods of seawater analysis*. John Wiley & Sons, 2009.

Mohrholz, V., Bartholomae, C.H., van der Plas, A.K., Lass, H.U. (2008) The seasonal variability of the northern Benguela undercurrent and its relation to the oxygen budget on the shelf, *Cont. Shelf Res.*, 28, 424-441.

Monteiro, P.M.S., van der Plas, A.K, Mélice, J.L., Florenchie, P. (2008) Interannual hypoxia variability in a coastal upwelling system: Ocean–shelf exchange, climate and ecosystem-state implications, *Deep-Sea Res.*, 55, 435–450.

Monteiro, P. M. S., van der Plas, A., Mohrholz, V., Mabille, E., Pascal, A., Joubert, W. (2006) Variability of natural hypoxia and methane in a coastal upwellingsystem: Oceanic physics or shelf biology?, *Geophys. Res. Lett.*, 33, L16614

Monteiro, P. M. S., et al. (2006) Variability of natural hypoxia and methane in a coastal upwelling system: Oceanic physics or shelf biology?, *Geophys. Res. Lett.*, 33, 16.

Naqvi, S. W. A., Bange, H. W., Farías, L., Monteiro, P. M. S., Scranton, M. I., and Zhang, J. (2010) Marine hypoxia/anoxia as a source of CH_4 and N_2O, *Biogeosciences*, 7, 2159-2190.

Wolk, F., Yamazaki, H., Seuront, l., Lueck, R.G. (2002) A new free-fall profiler for measuring biophysical microstructure, *J. Atmos. Oceanic Technol.*, 19, 780–793.

Xu, Z., Chang, P., Richter, I., Kim, W.-M. (2014) Diagnosing Southeast Tropical Atlantic SST and Ocean Circulation Biases in the CMIP5 Ensemble, *Clim. Dyn.*, 43, 3123–3145.

11 Appendix – List of Abbreviations

ADCP	Acoustic Doppler Current Profiler
ARGO	Array for Real-time Geostrophic Oceanography
BMBF	Federal Ministry of Education and Research
CH_4	Methane
CO_2	Carbon Dioxide
CTD/O_2	conductivity, temperature, depth and oxygen
FAO	Food and Agriculture Organization of the United Nations
lADCP	lowered acoustic Doppler current profiles
MSS	microstructure system
NatMIRC	National Marine Information and Research Center
NH_4^+	ammonium
N_2O	nitrous oxide
NO_3^-	Nitrate
NO_2^-	Nitrite
OMZ	oxygen minimum zone
OS	Ocean Surveyor
PAR	photosynthetically active radiation
PO_4^{3-}	phosphate
PREFACE	Enhancing prediction of tropical Atlantic climate and its impacts
RACE	Regional Atlantic Circulation and Global Change
SACUS	Southwest African Coastal Upwelling System and Benguela Niños
SSS	sea surface salinity
SST	sea surface temperature
SFB	collaborative research project
TKE	turbulent kinetic energy
TSG	thermosalinograph
uCTD	underway profiles of conductivity, temperature, and depth
UVP	underwater vision profiler
VMADCP	vessel-mounted acoustic Doppler current profiler